CFD MODELLING OF A NOVEL CLARIFIER DESIGN FOR USE IN SUGAR CANE JUICE CLARIFICATION

Thishen Govender

BScEng (Natal)

Submitted in fulfilment of the academic
requirements for the degree of
MScEng
in the
School of Chemical Engineering
University of KwaZulu-Natal, Durban

July 2008

ACKNOWLEDGMENTS

I would like to thank the following people and organizations for their contribution to this study:

Mr. CJ Brouckaert and Mr. SB Davis	Thank you for giving me the opportunity to undertake this MSc project. Your advice and guidance was invaluable.
Mr. W du Toit	For providing the laboratory scale clarifier, and assistance with the experiments.
My Family	Thank you for your support and motivation during difficult times.
Reshma Singh	Thank you for the words of encouragement, and for giving me the will to push forward.
My Friends	Thanks guys, for keeping me in high spirits.
Prelan Gounder	Thanks for your assistance with writing up, and finally completing this dissertation.
Sugar Milling Research Institute	For funding this study and assistance with the experimental work.
University of KwaZulu-Natal (Durban)	For the use of laboratory facilities.
Maidstone Sugar Mill (Tongaat)	For the assistance in the testing of the Magra Ultrasep.
Wiggins Wastewater Treatment Works	For the use of the turbidimeter.

ABSTRACT

The purpose of clarification in the sugar industry is to remove soluble, insoluble and colloidal matter from cane juice. Efficient clarification is required to produce high quality sugar and to prevent entrainment of solids in downstream equipment.

The objective of this study is to produce a Computational Fluid Dynamics (CFD) model of the Magra Ultrasep clarifier. This was accomplished by:

- Modelling the hydrodynamics of a laboratory scale clarifier in the Fluent CFD program.
- Incorporating the flocculation process into the CFD model.
- Performing experiments on a pilot scale clarifier to obtain parameter values for the flocculation model.

The hydrodynamic model of the clarifier showed the presence of a recirculation zone above the baffle plate. Particle injections using Fluent's discrete phase modelling option determined that particles within the size range of 100μm to 4mm would circulate in this region, forming the bed of floc particles required for the Magra Ultrasep to work efficiently.

The flocculation process in Fluent was represented using three different solid phases of different particle sizes. Small and medium sized particles were allowed to combine to form larger particles by changing the volume fractions according to three rate equations.

A fibre glass laboratory scale model was set up at Maidstone Sugar Mill and fed the same sugar cane juice that enters the Rapi-Dorr clarifiers. The experimental results were then fed into a simplified flocculation model in MATLAB.

An overall rate constant (k) of $5kg.m^{-3}.s^{-1}$ for the flocculation kinetic equation satisfied the experimental result.

DECLARATION

I hereby declare that all the work submitted within this dissertation, except where specifically acknowledged, is mine. This dissertation has not been submitted, in whole or in part, for a degree at another university or institution.

.....

Thishen Govender

LIST OF EQUATIONS

EQUATION NUMBER	EQUATION
2.1-1	$rate\ of\ flocculation = \alpha\beta(i,j)n_i n_j$
2.1-2	$\frac{dn_k}{dt} = \frac{1}{2}\sum_{i+j=k}\beta(i,j)n_i n_j - \sum_{i=1}^{\infty}\beta(i,k)n_j n_k$
2.1-3	$\beta = \left(\frac{3kT}{3\mu}\right)\left(\frac{1}{d_i}+\frac{1}{d_j}\right)(d_i + d_j)$
2.1-4	$\beta = \frac{1}{6}\left(\frac{du}{dy}\right)(d_i + d_j)^3$
2.1-5	$N_t = N_o \exp\left(\frac{4}{\pi}.\frac{du}{dy}\phi\, t\right)$
2.1-6	$\phi = \frac{4}{3}\pi a^3$
2.1-7	$\beta(i,j) = (G/6)(d_i + d_j)^3$

4.4.1-4 $$mass\ source = k_2 V_M^2$$

4.4.1-5 $$mass\ source = k_1 V_S V_M - k_2 V_M^2$$

4.4.1-6 $$mass\ source = -k V_S V_M$$

4.4.1-7 $$mass\ source = -k V_S V_M$$

4.4.1-8 $$mass\ source = 2k V_S V_M$$

4.4.3-1 $$C_D = \left(\frac{24}{\mathrm{Re}}\right)\left(1 + 0.14\,\mathrm{Re}^{0.7}\right)$$

4.4.3-2 $$u_t = \sqrt{\frac{4gd_p(\rho_p - \rho)}{3\rho C_D}}$$

4.4.3-3 $$settling\ factor = \rho_s A u_t$$

SYMBOLS

SYMBOL	DEFINITION	UNITS	EQUATION
a	particle radius	m	**2.1-5**
A	cross sectional area at the bottom of the bed	m^2	**4.4.3-3**
C	system constant	-	**2.1-13**
C_D	drag coefficient	Fraction	**4.4.3-1**
D	fractal dimension	-	**2.1-12**
d_p	particle diameter	m	**4.4.3-2**
du/dy	fluid velocity gradient	s^{-1}	**2.1-3**
e	floc porosity	Fraction	**2.1-12**
g	gravitational acceleration	$m.s^{-2}$	**2.1-7**

$\mathbf{S}$	system constant	-	**2.1-12**
$\mathbf{T}$	temperature	K	**2.1-3**
$\mathbf{u_t}$	terminal settling velocity	$m.s^{-1}$	**4.4.3-2**
$\mathbf{V_L}$	volume fraction of large secondary phase	Fraction	**4.4.1-1**
$\mathbf{V_M}$	volume fraction of medium secondary phase	m^3	**4.4.1-3**
$\mathbf{V_S}$	volume fraction of small secondary phase	Fraction	**4.4.1-1**
$\mathbf{v_{sj}}$	the settling velocity of the solids in layer j	$m.s^{-1}$	**2.1-14**
$\mathbf{v_u}$	underflow velocity	$m.s^{-1}$	**2.1-14**
$\mathbf{x}$	system constant	-	**2.1-13**
$\mathbf{X_j}$	solids concentration in layer j	$kg.m^{-3}$	**2.1-14**
α	collision efficiency	Fraction	**2.1-1**

LIST OF FIGURES AND GRAPHS

CONTENTS

CHAPTER 1 INTRODUCTION

This chapter presents the background of the project, along with the scope of work. This is followed by a summary of the thesis chapters and an outline of how they link up. Also included is a flowsheet representation of the thesis outline, shown on page 1-4 (Figure 1-1).

1.1 BACKGROUND

The Magra Ultrasep clarifier is a relatively new design that is currently being used in the minerals industry. The Sugar Milling Research Institute (SMRI) wanted to use CFD modelling to determine if the advantages of this new design can be realised in the sugar cane juice clarification process. The SMRI funded this MSc project at the University of Kwa-Zulu Natal in order to achieve this, and a laboratory scale clarifier was supplied by Mr W. du Toit.

Some of the more important, potential advantages of the Magra Ultrasep are:

- Quick response to changing feed conditions.
- High capacity per square area
- Reduced flocculant consumption

Refer to 3.1 (on page 3-1) for a detailed explanation of the operation of the Magra Ultrasep.

1.2 PROJECT SCOPE

The following work was conducted during this study:

1.2.1 CFD MODELLING

A Computational Fluid Dynamics (CFD) model of the clarifier was constructed in the Fluent program. It began with modelling the hydrodynamics and then developed into a multiphase model to include flocculation and settling of solids. The main aims were:

- To create a CFD model of the Magra Ultrasep clarifier illustrating the working principle of this new design i.e. the bed of flocculated particles.
- To then use the model to predict the performance of the clarifier.

- **Chapter 5: Discussion**

  This is essentially a summary of the discussions of results in the preceding **Experimental** and **Fluent Model Development** chapters (**Chapter 3** and **4** respectively).

- **Chapter 6: Conclusions and Recommendations**

  This chapter lists the final outcomes of the project followed by the recommendations for the further advancement of this work.

CHAPTER 2 LITERATURE SURVEY

The Magra Ultrasep 2000 High Performance Thickener serves as a thickener and a clarifier. The two operations occur simultaneously in this equipment to achieve liquid-solid separation. The purpose of thickening is to increase the concentration of suspended solids of the feed, while clarification is the removal of the solid particles resulting in a clear effluent (Perry and Green (1997)). However, before this operation can be understood, an explanation of the flocculation/coagulation process, which is at the heart of this unit operation, is required.

2.1 CLARIFICATION

There are different types of clarifier. The *clarifier-thickener* acts as a thickener as well as clarifier. A thickener, concentrates the suspended solids from a feed using gravity settling. This particular clarifier produces a dense sludge which is normally removed continuously. A *solids-contact* clarifier combines the operations of mixing, flocculation and sedimentation in a single unit. Flocculant is dosed into the feed as it enters the unit. Settled solids are recirculated via a draft tube inside the reaction well, and these meet with the solid particles in the feed, improving sedimentation.

Since the Magra Ultrasep is to be adapted for the sugar industry, knowledge of the specific methods used by sugar mills for the clarification of mixed juice is required. A summary of the sugar clarification module prepared by the Sugar Milling Research Institute can be found in Appendix F.

2.2 FLOCCULATION MODELLING

The following sections present some of the theoretical and numerical methods used to qualify the flocculation process.

2.2.1 CLASSICAL FLOCCULATION THEORY

Coagulation is the physicochemical process of combining of solid particles to form larger aggregates. It can be divided into two parts: particle destabilisation and flocculation. Four different mechanisms can result in particle destabilisation:

Smoluchowski (1917) was the first to attempt the modelling of the flocculation process, which resulted in the following equation:

$$\frac{dn_k}{dt} = \tfrac{1}{2}\sum_{i+j=k}\beta(i,j)n_i n_j - \sum_{i=1}^{\infty}\beta(i,k)n_j n_k \qquad 2.1\text{-}2$$

Particles of size i and j combine to form a particle of size k. The first summation term represents the increase in the number of particles of size, while the second summation term incorporates the loss of particles of size k due to aggregation. Smoluchowski used this expression to obtain a series of differential equations for different values of k. In order to solve these equations, he made some simplifying assumptions:

1. The collision efficiency factor α is ignored (α = 1)
2. Fluid motion undergoes laminar shear
3. Particles are all of the same size (k)
4. All particles are spherical
5. Floc breakage is ignored
6. Collisions involve two particles at a time

The resulting analytical expressions for collision frequency were:

Perikinetic flocculation: $\beta = \left(\frac{3kT}{3\mu}\right)\left(\frac{1}{d_i}+\frac{1}{d_j}\right)(d_i + d_j)$ 2.1-3

Orthokinetic flocculation: $\beta = \tfrac{1}{6}\left(\frac{du}{dy}\right)(d_i + d_j)^3$ 2.1-4

where: k is Boltzmann's constant

T is bulk liquid absolute temperature

μ is the fluid viscosity

du/dy is the fluid velocity gradient

The analytical solution to equation 2.1-2 for both perikinetic and orthokinetic flocculation was found to be:

$$N_t = N_o \exp\left(\frac{4}{\pi}.\frac{du}{dy}\phi\, t\right) \qquad 2.1\text{-}5$$

with

$$\phi = \tfrac{4}{3}\pi a^3 \qquad 2.1\text{-}6$$

particle sizes. The drag on aggregates in a flow field was examined considering porosity (both uniform and non-uniform) and the paths adopted by particles approaching each other.

2.2.1.2 FLUID MOTION

Smoluchowski (1917) concluded that the rate of orthokinetic flocculation was proportional to the velocity gradient based on the fluid motion being laminar. Camp and Stein (1943) proposed that flocculation rate was dependent on a term (G) that they defined to be the local root mean square velocity gradient of the fluid for three-dimensional fluid motion. They also found that G was related to the local energy dissipation rate (ε):

$$G = \left(\frac{\varepsilon}{\nu}\right)^{0.5} \qquad 2.1\text{-}9$$

where: ν is the kinematic viscosity of the fluid.

This expression was modified, using an average energy dissipation rate to obtain the average G (global root mean square velocity gradient), which was then used for turbulent fluid flow.

2.2.1.3 PARTICLE SIZE DISTRIBUTION

Assuming that all the colliding particles are of the same size (monodispersed), greatly simplified the flocculation equations allowing an analytical solution to be found. Using the G term defined by Camp and Stein, the orthokinetic flocculation equation (Equation 2.1-5) becomes:

$$N_t = N_o \exp\left[-\frac{4Gt\alpha\phi}{\pi}\right] \qquad 2.1\text{-}10$$

Initially, the dimensionless term, Gt, was considered to be the principal design parameter to be used to determine flocculation progress. The design parameter was proposed to be Gtf by Tambo (1965) and then Gtfa by O`Melia (1972). The effect of larger aggregates becomes significant as flocculation progresses, making the assumption of a monodispersed system suitable only in the initial phase of the flocculation process.

In heterodispersed systems, the size distribution of particles can be described as either continuous or discrete. Initially, discrete functions were arithmetic series, but the number of particle sizes increases greatly with increasing size ranges. Geometric series were tried next, but this series provided less information than the arithmetic series. Eventually, instead of

2.2.1.5 FLOC BREAKAGE

Spicer and Pratsinis (1996) showed that the phenomena of floc breakage and aggregation determine the size and mass distribution of solids. Simulations by Costas et al. (1995) demonstrated that reaction rates and final size distributions were quite sensitive to assumptions about break-up mechanisms. Initially, breakage was thought to be dependent on floc size. However, it was later found that floc compactness was of more importance. An empirical dependence of maximum floc size on G (the root mean square velocity gradient) was found by Ritchie (1955). This implied the existence of a critical G, above which, effective flocculation rate would decrease. Tambo and Hozumi (1979) formulated the following equation:

$$maximum\ floc\ size = C(G)^{-x} \qquad 2.1\text{-}13$$

where: C and x are constants.

Subsequent research resulted in the inclusion of the effects of floc strength, primary particles size and mixing intensity in Equation 2.1-13.

2.2.1.6 COLLISIONS OCCUR BETWEEN TWO PARTICLES AT A TIME

With highly concentrated suspensions, there is a greater likelihood that more than two particles will collide at a time to form a larger floc particle. Thermodynamic theory of flocculation is where stabilised and destabilised colloids are considered to be the liquid and solid phases respectively. Rajabopalan (1993) found that phase diagrams for a model with solids considered to be adhesive hard spheres, were close to those obtained assuming short range attractive forces. This model provided a way of determining the degree of destabilisation required for flocculation to occur.

2.2.2 NUMERICAL MODELLING OF THE FLOCCULATION PROCESS

Takacs (1991) modelled the clarification-thickening process in a settling column. A simple model was constructed by dividing the vessel into a finite number of layers. It was assumed that solids are distributed evenly within each layer, and as such, only vertical flows are considered. The model simulates the solids concentration profile within the column by adhering to solid flux and mass balances around each layer:

$$J_j = X_j v_{sj} + X_j v_u \qquad 2.2\text{-}14$$

obtained using particle image velocimetry (PIV). Flocculation experiments were conducted in an agitated vessel using a bentonite suspension, where a laser illuminates the vessel, and a camera captures a two-dimensional image of the suspension. Thereafter, pattern recognition software is used to analyse the image, providing the floc size distributions at various times. It was found that the mean area occupied by the flocs reached steady state within shorter times with increasing impeller speeds. However, the maximum floc size decreased with increasing impeller speed. PIV provided information on local velocities allowing the mean velocity gradient (G) to be determined. It was discovered that instantaneous velocity gradients reach a maximum shortly after on of the impeller blades passes through that region, and can be up to six times the averaged value. Furthermore, using two different methods, the maximum floc size was found to relate to the average energy dissipated in the vessel.

Population balance modelling (PBM) is a method where particles are categorised into different groups based on their size. Floc growth will result in a particle moving from one size group to the next. The difficulty with such a model is that the size and number of particles needs to be precisely known at various times. Nopens et al. (2002) used PBM together to model the activated sludge flocculation process. Laser light diffraction was then used to measure floc size distribution on sonicated sludge. The model prediction for steady state mean floc size was generally lower than experimental. The authors alluded to further work involving the use of PBM together with CFD to create a more complete model.

2.3 CFD MODELLING

Computation fluid dynamics (CFD) is a predictive tool that is used to analyse fluid flows. Its fairly recent practicability is due to the ever-increasing computational speed of computers. The inputs required are a two, or three-dimensional geometry and the boundary conditions of the system. The geometry is divided into discrete elements, and the solution that satisfies the mass, momentum and heat transfer equations is found by iteration. In this way, complex systems can be modelled. The CFD model can then be used to predict the behaviour of the system allowing for quick and effective optimisation. The operational characteristics of a particular design or system can be analysed without having to build large-scale test units. The papers presented help illustrate the use of CFD as well as the growing complexity of the models.

Ta, Beckley and Eades (2001) investigated the operation of a dissolved air flotation tank using a 3-D multiphase CFD model. Floc particles were then injected into the model to ascertain the trajectory and fate of the flocs, depending on size and density.

Greene, Haas and Farouk (2002) simulated a continuous flow pilot scale chlorinator. The model was first validated, and then used to show the effect of inlet configurations on reactor hydrodynamics.

Salter, Ta and Williams (2000) reviewed the design of a series of facultative lagoons in Thailand with a view to improve biological oxygen removal. CFD modelling showed that the lagoons were experiencing significant short circuiting and contained large dead zones. Furthermore, the model demonstrated that the installation of baffles increase retention time and consequently improve performance.

De Kretser, Mathews and Williams (2003) compared the degree of mixing in aerators with that of mixers. The aim was to establish whether mixers could replace the aerators installed in an Australian lagoon. The CFD model agreed with physical experimental results in showing that short-circuiting occurred along the dividing wall. According to the final CFD results, the optimal solution would be to use alternate aerators and mixers together.

Kamimura, Furukawa and Hirotsuji (2002) combined a complex radical reaction model with CFD in order to simulate an ozone/UV contactor. The model successfully calculated the concentrations of TOC, H_2O_2 and dissolved ozone for a lab scale model. Thereafter, the concentrations of the hydroxyl radical (·OH), H_2O_2 and ozone in the reactor were predicted.

Brannock et al. (2002) included particulate settling and biological reactions (based on Activated Sludge Model No. 1) in a CFD model of a wastewater treatment reactor. Results were verified by tracer tests.

de Clercq (2003) presented a CFD model of a settling tank which incorporated sub-models for solids sedimentation, sludge rheology and a scraper mechanism.

Dahl et al. (1994) created a two-dimensional model of a rectangular tank using PHOENICS software. Experiments were then conducted on a prototype clarifier in order to calibrate the model. The velocity distribution and suspended sludge concentration were sufficient for successful model calibration.

Zhou and McCorquodale (1991) mathematically modelled flows in a secondary clarifier. The model was then used to predict the concentration distributions of a non-uniform flocculated suspension. They then constructed and solved a two-dimensional model of the clarifier, complying with the k-ε turbulence model and mass and momentum conservation equations.

In a later study, Zhou and McCorquodale (1992a) looked at solids settling at the inlet of a circular clarifier. They developed a numerical model to predict solids concentrations within the tank. The flow was assumed to be a single phase with stratified density. Viscosity was evaluated using the k-e turbulence model, while the mass and momentum equations were used to solve the unsteady turbulent flow. The model results compared well with experimental data.

Zhou and McCorquodale (1992b) then investigated a rectangular clarifier. Models were developed for a clarifier both with and without baffles. Experimental results for both cases were obtained on three different sized tanks. These agreed well with the model with respect to flow patterns. No experiments were conducted to confirm the concentration profiles. These results were compared to results from a theoretical method developed by Takacs et al. (1991).

Zhou, McCorquodale and Vitasovic (1992) tested the effects of baffles under varying conditions using a numerical model. The solids and hydraulic loads were varied and found to be affected by the densimetric Froude number. Experiments with varying flow rates together with a dye test confirmed the model predictions.

Following on this, Zhou and McCorquodale (1993) applied the same numerical model to a circular clarifier without baffles. This time, the effect of both Froude number and Reynolds

Continuing with this study Steindl (1998) used the FIDAP CFD model to identify and analyse the operation of the SRI clarifier, with the intent of improving the design. The FIDAP model showed a significant short-circuiting of mixed juice from the exit of the feed well to overflow launder. A modification was made to allow the feed to enter at the periphery with the overflow exit to be at the center. The model showed that this design would achieve low fluid velocities in the settling region, which would substantially improve performance. The CFD model was validated using tracer tests. Here, the residence time distribution curves obtained from experiment were compared to a simulated test (on the CFD model). The modified SRI clarifier was installed during Australia's 1997 season and performed well, operating at 50% above the initial design loading.

Peacock et al. (2000) modelled a Rapidorr 444 clarifier using the Fluent computational fluid dynamics program. The purpose of the study was to obtain a better understanding of the fluid behaviour within the compartments of the clarifier, and later, evaluate the effect of geometrical changes on clarifier performance. Various approximations were made to create a two-dimensional, axisymmetric model of the Rapidorr in Fluent. The boundary conditions of feed rate, viscosity, density, mud underflow rate and mud particle density were entered into the program. The modelling results showed the presence of a recirculation zone near the floor of the vessel, as well as a region of upward velocities near the inlet of the clarifier, both of which would negatively affect particle settling. The effects of five baffles in various positions were investigated, and one was found to be promising. However, this modification was found to be impractical to implement. In order to increase the reliability of the model, a three-dimensional was to be investigated in the future.

Chetty et al. (2001) continued with the study, and created a three-dimensional model of the Rapidorr clarifier. Comparison of this model with the previous one, showed that the two-dimensional, axisymmetric model was just as accurate as a three-dimensional one, implying that the boundary conditions and assumptions made were acceptable. The CFD model was validated performing tracer tests, and comparing experimental residence time distribution curves with simulated ones. Using Fluent, geometrical changes to the clarifier were assessed. It was found that a combination of baffles placed in two specific positions would produce a desirable flow pattern, and resulting in improved mud settling. However, the

CHAPTER 3 EXPERIMENTAL

The practical application of this design was conducted on a laboratory scale clarifier, provided by W. du Toit of Magrasaver (Pty) Ltd. Experiments on this piece of equipment were undertaken for two main reasons. Firstly, a practical evaluation of the clarifier would provide an indication as to whether or not the clarifier can perform its desired function adequately. Secondly, experiments would produce the data required to calibrate and test the Computational Fluid Dynamics (CFD) model of the clarifier.

3.1 THE WORKING PRINCIPLE OF THE MAGRA ULTRASEP

Constructed of fibreglass, the clarifier (Figure 3.1-2) stands just over 2m high and has an inner diameter of 27 cm. At the bottom, there are three support legs along with two outlets. The outer shell has three perspex windows on the side, and a toothed weir with an overflow tray at the top (Figure 3.1-3). The insides comprise of an annular mixing chamber, the dewatering pipe connected to the collector cone, a conical baffle (Figure 3.1-4) and three toroidal consolidation cones (Figures 3.1-5). Three support arms extend radially outwards from the dewatering pipe, through the mixing chamber, to suspend the internals via three fibreglass blocks on outer shell.

Refer to Figure 3.1-1 (taken from a presentation of the Magra Ultrasep sourced from W. du Toit). The flocculated feed enters the annular mixing chamber and moves downward to the sixty degree collector cone. The cone deflects the feed, distributing the solids within the free settling zone. Large flocs sink and approach the consolidation cones. These cones are toroidal in shape with a triangular cross section. Particles slide or roll down the inclined surfaces causing liquid entrained between particles to be displaced, increasing underflow density. Some of the displaced liquid rises to the free settling zone while the rest moves up the centre axis into the dewatering pipe. This liquid carries with it small solid particles that enter the mixing chamber, providing seeding flocs for the feed which improves flocculation. The smaller flocs, that enter the free settling zone, rise up the outer annulus, where they encounter the conical baffle. The baffle increases the fluid's upward velocity by reducing the cross-sectional area. Thereafter, upward velocity decreases as area increases. Consequently, flocs within a certain size range will initially move upwards, gradually

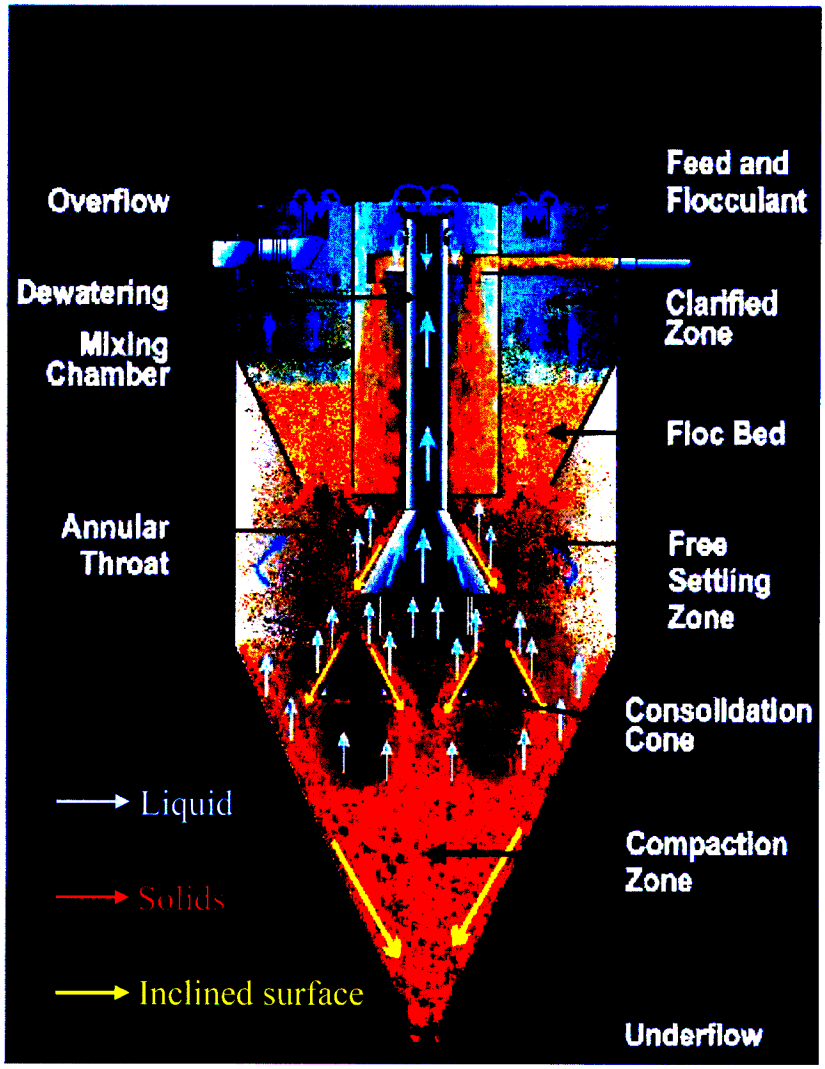

Figure 3.1-1: Operation of the Magra Ultrasep

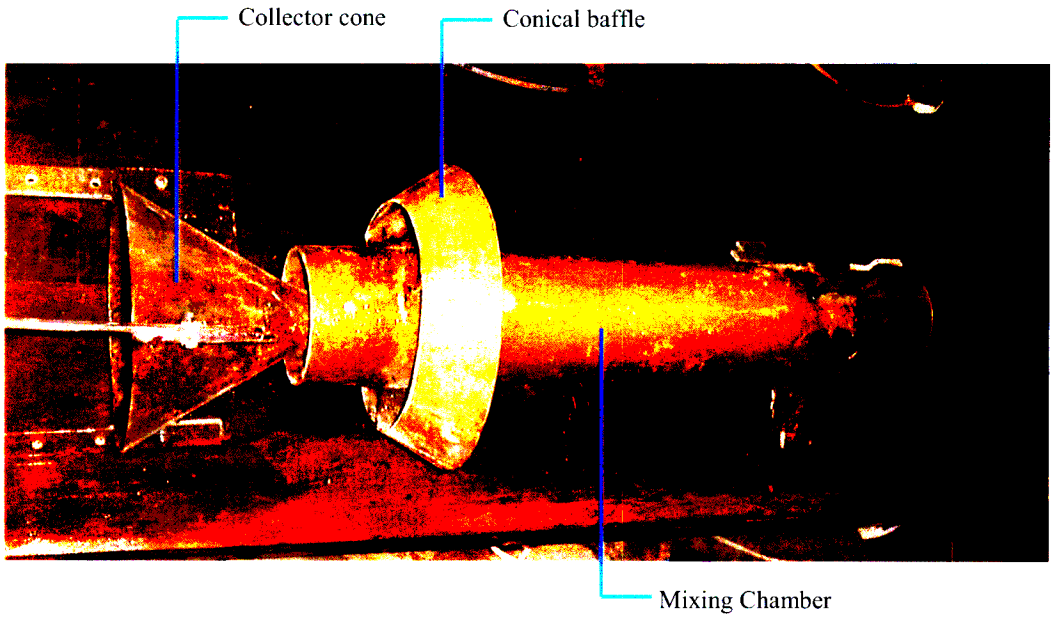

Figure 3.1-4: Upper Section of Clarifier Internals

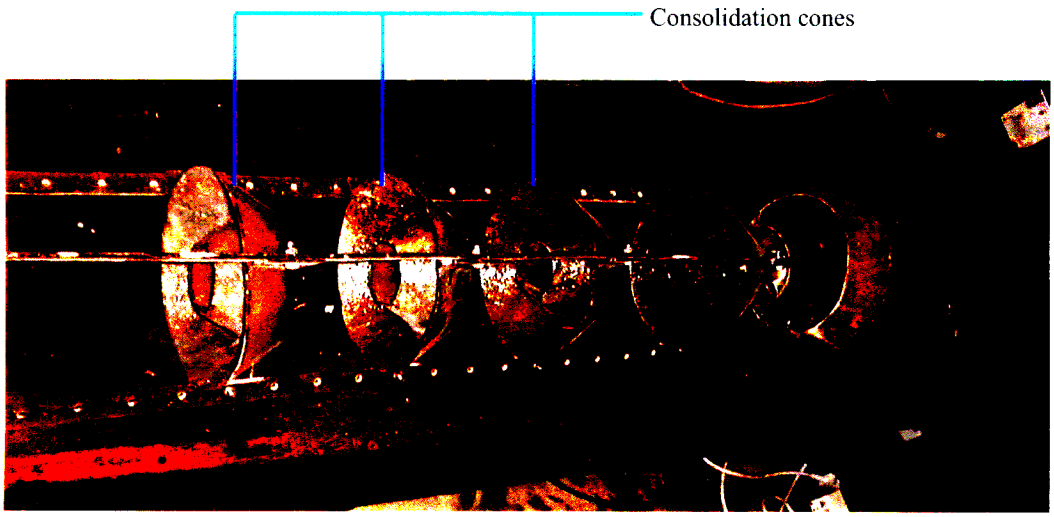

Figure 3.1-5: Clarifier Internals

3.3 MAIDSTONE 2002

The laboratory scale Magra Ultrasep clarifier was set up at Maidstone Sugar Mill to assess its operation.

3.3.1 EXPERIMENTAL SETUP

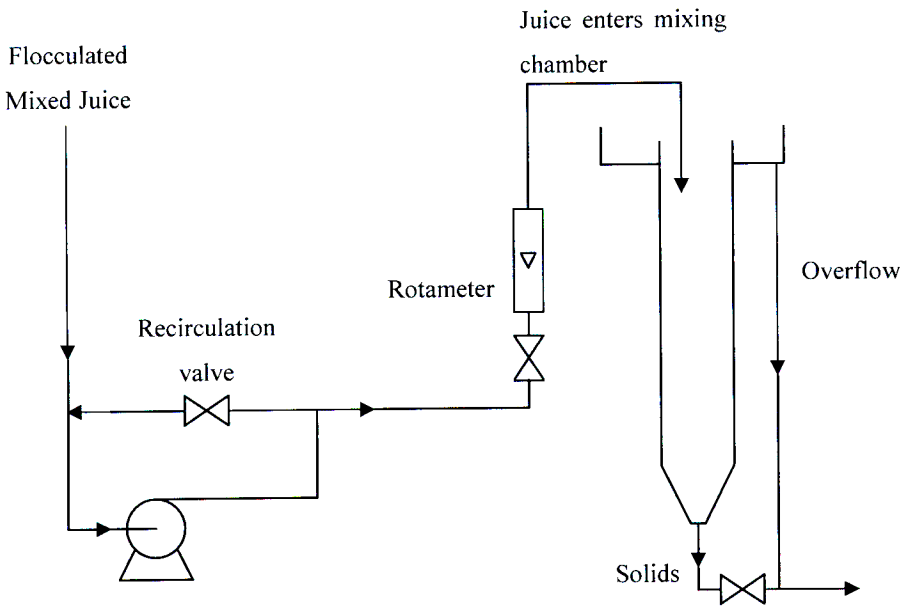

Figure 3.3-1: Pilot Plant at Maidstone Mill (November 2002)

Flocculated mixed juice was drawn from the feed line to one of the Rapi-Dorr type clarifiers currently in operation at the mill. A recirculation line with a valve was required in parallel with the positive displacement pump for flow rate control. Measurement of this flow rate was achieved using a rotameter. Mixed juice enters the inlet annulus at the top clarifier, while clarified juice exits from the overflow at the top. Solids that collect at the bottom were not removed continuously, but rather, between runs.

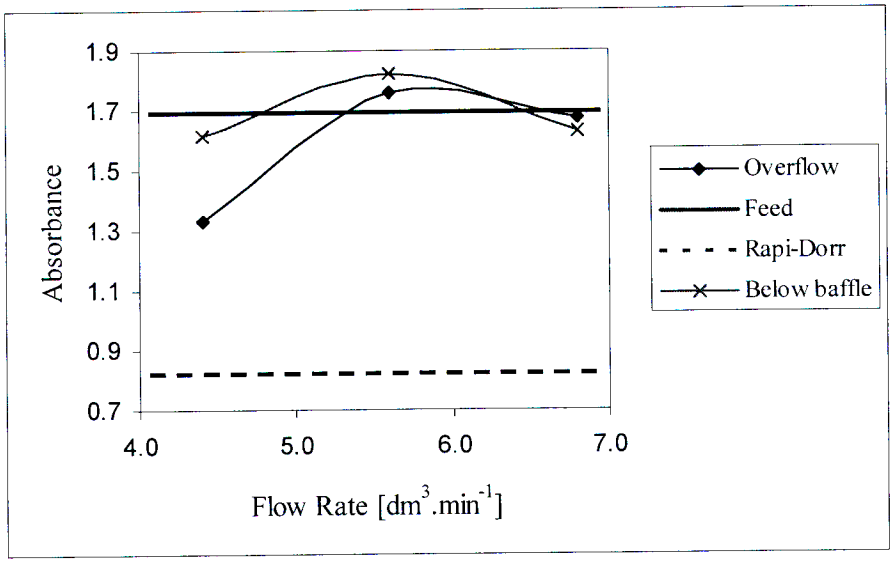

Graph 3.3-2: Absorbances of the Overflow and Below the Baffle (03-11-2002)

3.3.4 DISCUSSION

The absorbance of the Magra Ultrasep overflow remained below that of the feed, with the exception of a few isolated cases. This indicates that solids are settling within the vessel. However, the absorbance of Maidstone's Rapi-Dorr clarifier overflow was consistently lower than that of the Magra Ultrasep clarifier, even when the latter was run at low flow rates of about 3 to 4$dm^3.min^{-1}$. In most cases, the absorbance of the sample from below the baffle was higher than the overflow. The calibration graph data (Graph A-1) is considerably scattered (R^2 = 0.84). One of the factors affecting this is the solids settling in the cuvette, while the spectrophotometer is measuring the absorbance. Although agitation prior to measurement results in floc breakage, the flocs can quickly reform resulting in an absorbance that does not reflect the actual solids content. Therefore, a more reliable measurement technique or apparatus is required.

During the runs, it was observed that the rotameter float sometimes became stuck as larger flocs were unable to pass through the gap between the float and rotameter wall. The rotameter was subsequently reconnected to measure the overflow flow rate, as opposed to inlet flow rate. The measurement itself was now more reliable, but changes in inlet flow rate were not immediately reflected in the rotameter reading.

solution is formed. The addition of a base, to increase the pH to anywhere between 6 and 9, causes aluminium hydroxide ($Al(OH)_3$) to precipitate. This flocculating system was then used in a series of experiments on the Magra Ultrasep clarifier.

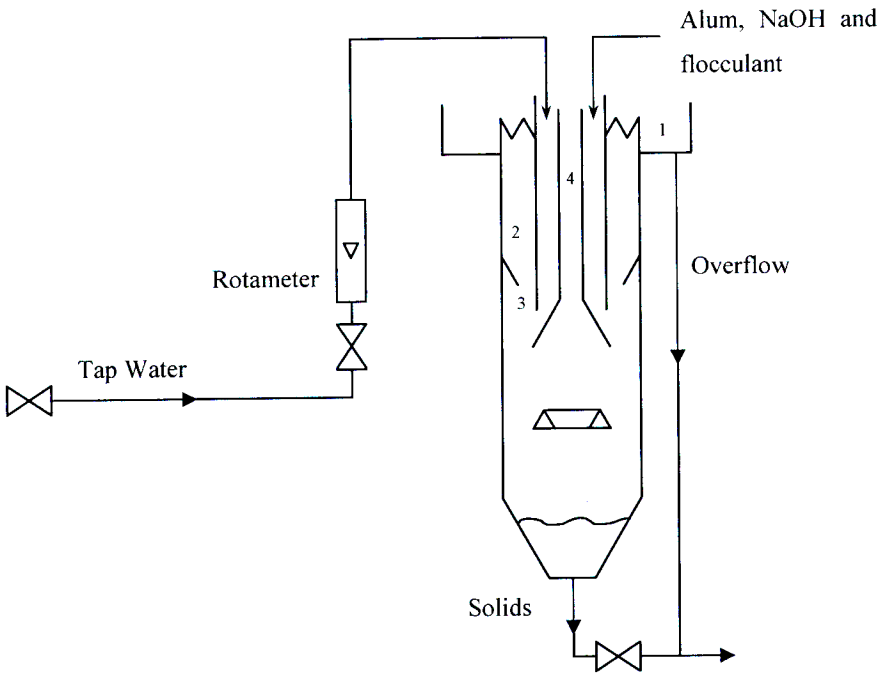

Figure 3.4-1: Clarifier Configuration for Alum Experiments

The Magra Ultrasep was now set up in the Biochem Laboratory in the Chemical Engineering building of the University of Kwa-Zulu Natal. Tap water, which is now the bulk liquid, is fed into the mixing chamber via the feed pipe connected directly to the tap fitting. Medical drip bags ($1dm^3$ capacity) suspended about 1m above the clarifier supplied alum, sodium hydroxide and flocculant to the clarifier.

3.4.1 EXPERIMENTAL PROCEDURE

Firstly, the feed solutions of alum (33g alum in $1dm^3$ of water), NaOH ($0.28mol.dm^{-3}$) and flocculant (0.1g of LT27 in $1dm^3$of water) were prepared. The NaOH and flocculant form homogenous solutions, but the alum, at this concentration, does not dissolve completely. The result is a suspension of fine particles. However, the consistency of this formulation was reasonably constant over the duration of one experimental run.

Figure 3.4-2: Top Sight Glass 5 minutes After Seeding

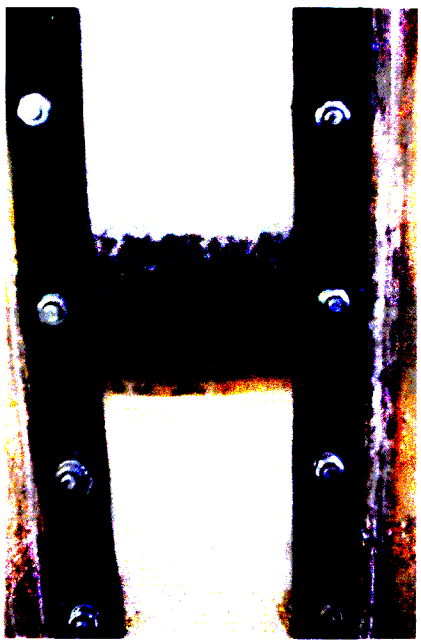

Figure 3.4-3: Middle Sight Glass – Large Flocs Falling

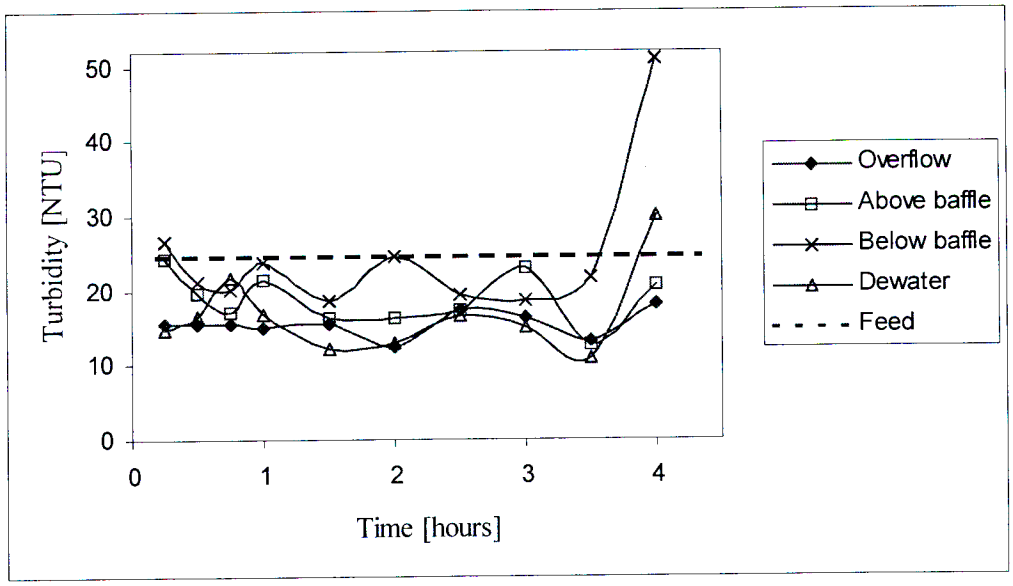

Graph 3.4-2: Turbidity Profiles within the Magra Ultrasep for a 4 hour run (21-07-2003)

3.4.4 DISCUSSION

As was expected, almost all the run show an initial decrease in solids concentration at the overflow and above the baffle. This is due to the addition of seeding flocs in this region. In the 30 minute runs, the turbidity of the region below the conical baffle seemed to exceed that of the other regions by a substantial amount, in one sample set only (Graphs B-2 to B-6). This phenomenon is also observed in the one hour run without dosing (Graph B-11). For the most part, the turbidities in all four regions seemed to follow the same trend (i.e. a general increase or decrease), although their relative positions were not always the same. In most cases, the solids concentration below the baffle was the highest, but this was not always the case. The seemingly random occurrence of high turbidity below the baffle, suggests the possibility of a bed of flocs forming in this region that can only be maintained for a short time period.

Observation of the behaviour of this particular flocculating system in the clarifier, revealed that during some runs, even large flocs rise past the conical baffle. Upon closer examination, the flocs seemed to have air bubbles trapped within them, which would have contributed

3.5.2 EXPERIMENTAL SETUP

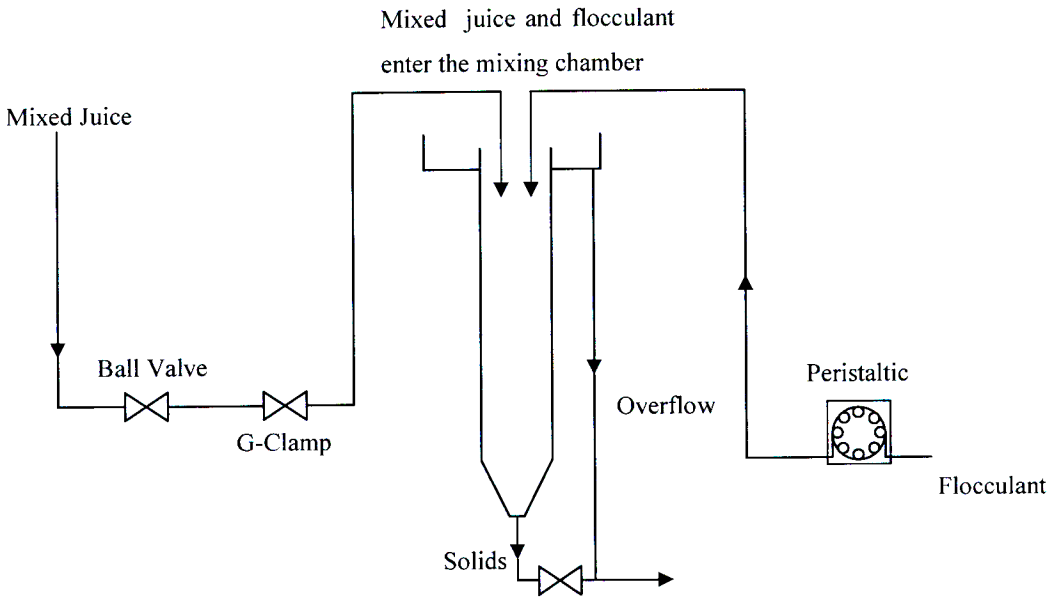

Figure 3.5-2: Experimental Setup at Maidstone

Refer to Figures 3.4-1 and 3.4-2. Unflocculated mixed juice was fed to the mixing chamber via one inch rubber hosing. The ball valve placed on this line was kept fully open during an experimental run. The flow rate was monitored with a bucket and a stopwatch at the outlet end, and controlled using a G-clamp on the inlet line. This decreased the occurrence of solids (mud and fibres) entrainment in the line fittings. Flocculant was dosed directly into the mixing chamber with a peristaltic pump.

3.5.3 EXPERIMENTAL PROCEDURE

The clarifier was run at $9dm^3.min^{-1}$. At Maidstone, a 0.05% flocculant solution is prepared and dosed to a final concentration (in mixed juice) of 3 to 7ppm. For this experiment, the flocculant had to have a higher concentration since it was being dosed by a low capacity peristaltic pump. Therefore a flocculant solution was mixed to 1.25% concentration (12.5g

Figure 3.5-3: Experimental Setup at Maidstone

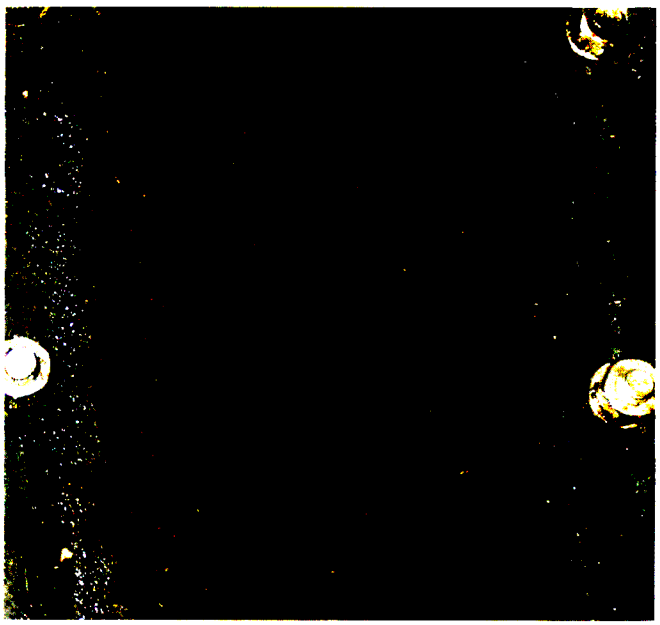

Figure 3.5-4: Top Sight Glass Showing Sludge Bed

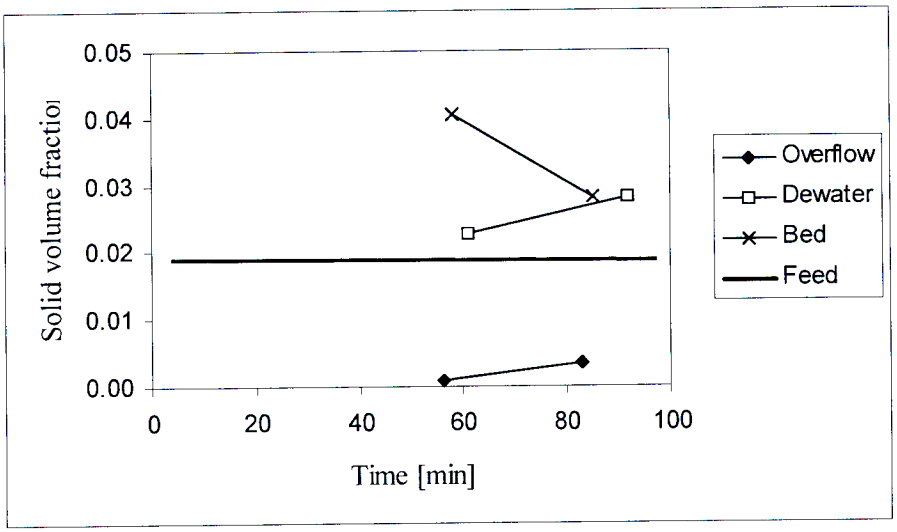

Graph 3.5-3: Volume Fraction Profiles (20-11-2003 – run 1)

3.5.6 DISCUSSION

In all cases, the solids present in the overflow, was lower than the feed, implying that solids were settling within the clarifier. Overflow solid volume fraction ranged were usually low, but varied greatly with each experimental run (0.0004 to 0.04). However, the Rapi-Dorr clarifier consistently outperformed the Magra Ultrasep, with a maximum overflow solids volume of 0.002, for the duration of the testing.

Occasionally, the region was filled with solids, as seen in Graphs 3.5-2, and C-6. However, the solids collected to form a sludge-like mass of mud, instead of the expected bed of solids suspended by the flow. This could mean that the flocculant dosage was too high, even though the ratio of flocculant to feed was half that of the Rapi-Dorr clarifier.

The erratic nature of the Magra Ultrasep's performance on mixed juice, as well as the sludge bed phenomenon rendered most of the data as unreliable. Consequently, the data from one run (20-11-2003 run 1 – Graph 3.5-3) was used to determine the Matlab model parameters. On this run, the sludge bed did not form and the overflow solids volume fraction remained

CHAPTER 4 FLUENT MODEL DEVELOPMENT

The Magra Ultrasep clarifier has many interrelated processes occurring simultaneously. The Computational Fluid Dynamics (CFD) package Fluent was utilized in an attempt to produce a working model that incorporates all these processes.

4.1 SOLVING THE FLOW FIELD

The first step was to input all the known data of the system into the Fluent package and construct a model. The geometry as well as known physical properties were used to solve the hydrodynamics of the laboratory Magra Ultrasep clarifier.

4.1.1 GEOMETRICAL SIMPLIFICATIONS

Physical measurements of the clarifier provided the basis for the geometry of the Fluent model. The mesh was created using the Gambit package. Certain geometrical simplifications were made in order to decrease the computational load of the model, hence reducing the time required for the solution to converge.

Figure 4.1-1 shows the clarifier model geometry. The axial symmetry of the clarifier allowed an axisymmetric, two-dimensional model to be used. The model was adapted to cater for certain features of the design that were not axially symmetric. The feed pipe is a single length of pipe protruding downwards into mixing chamber, but was modelled as an annular inlet. The clear overflow exits the clarifier by flowing over a toothed weir, into a tray and finally through a single outlet pipe. For the model, part of the clarifier wall was set to be an outlet edge, facing radially outwards. The overflow is exposed to air when flowing over the weir, and if this was to be taken into consideration, another phase (gas) would be required, significantly increasing the computational load of the simulation. It is reasonable to assume that the ambient air should be sufficiently quiescent not to have any real effect on clarifier, and consequently, an edge with a roughness coefficient and a roughness height of zero (an essentially frictionless surface) was placed above the outlet edge. The model did not require a bottom outlet since, during clarification, mud is not removed continuously. Practically, mud that accumulates at the bottom is removed periodically. The feed annulus,

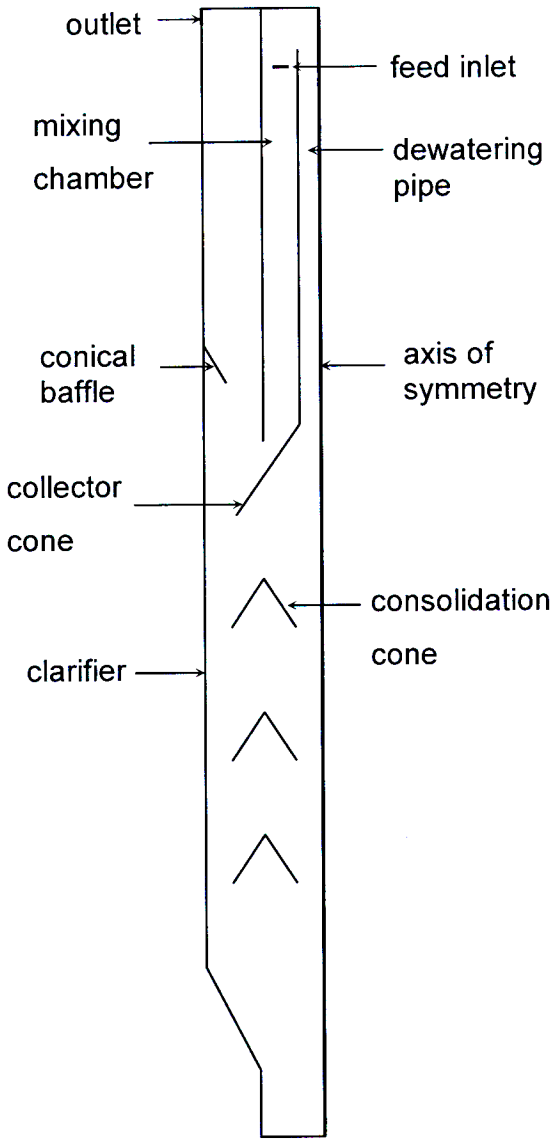

Figure 4.1-1: Fluent Model Geometry

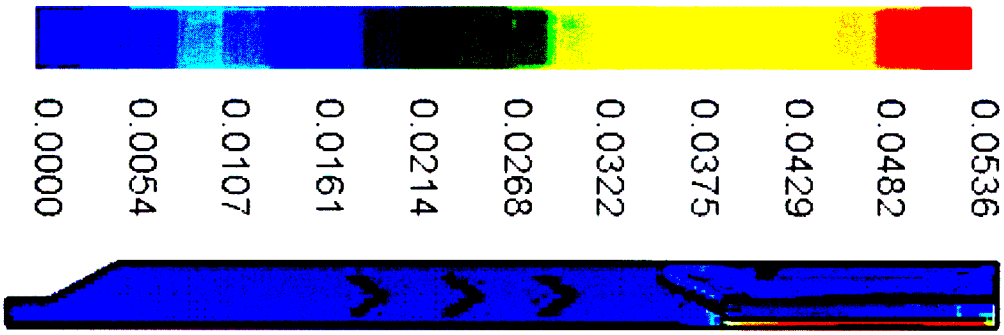

Figure 4.1-2: Clarifier Hydrodynamics – Velocity Countours ($m.s^{-1}$)

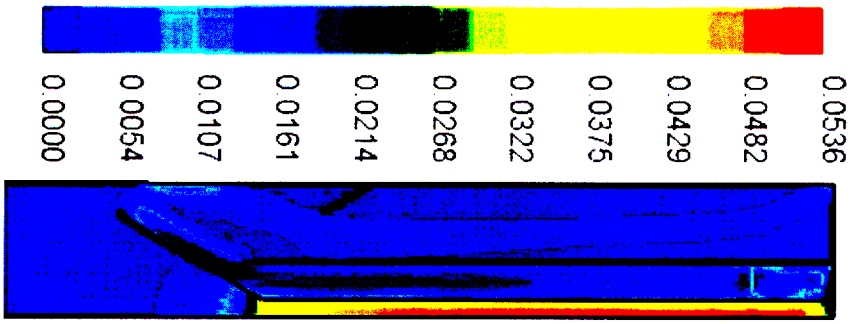

Figure 4.1-3: Clarifier Hydrodynamics (Upper Section) – Velocity Contours ($m.s^{-1}$)

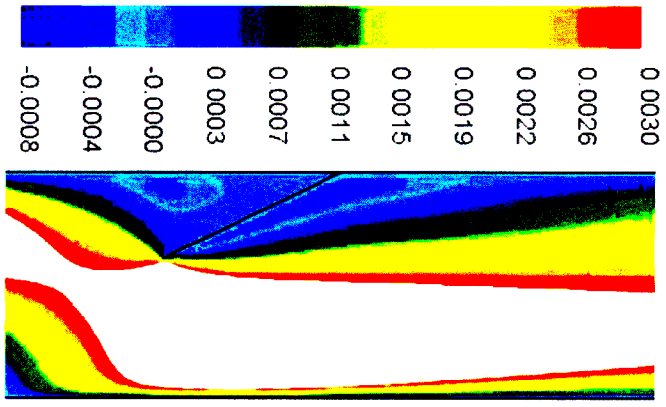

Figure 4.1-4: Bed Region (Upper Section) – Axial Velocity Countours ($m.s^{-1}$)

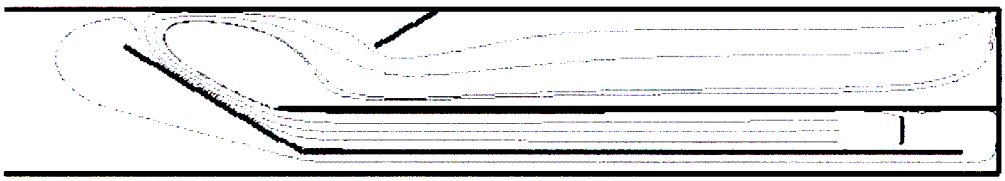

Figure 4.2-1: DPM – 100µm particle paths

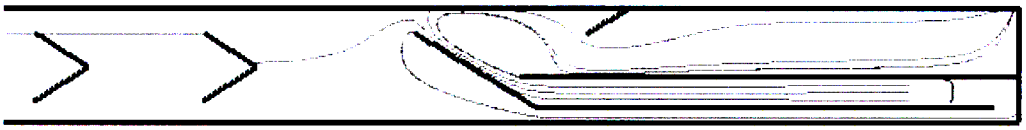

Figure 4.2-2: DPM – 1mm particle paths

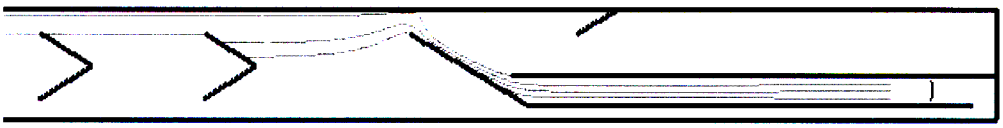

Figure 4.2-3: DPM – 1.8mm particle paths

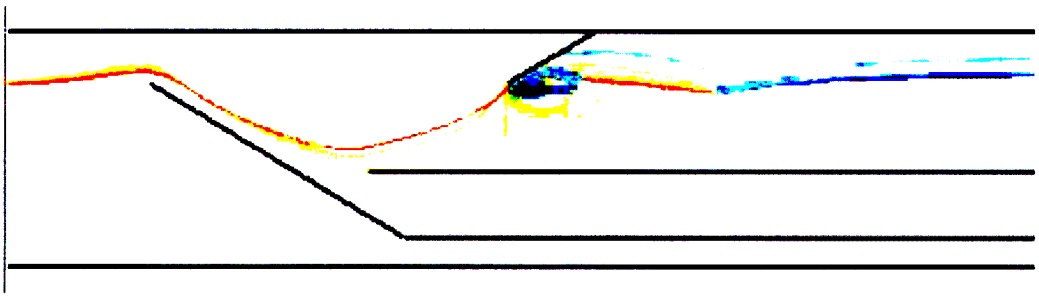

Figure 4.2-4: DPM – 8 particle paths (100µm to 4mm)

4], and [4.3-5, 4.3-6] show the solid volume fraction profiles followed by the corresponding velocity contours for particle diameters of 100μm, 800μm and 3mm respectively, after an iteration time of just over two hours has elapsed.

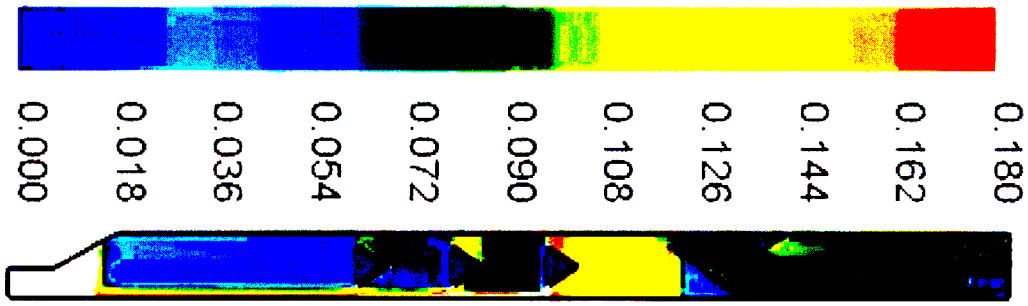

Figure 4.3-3: Volume Fraction Profile of 800µm Particles

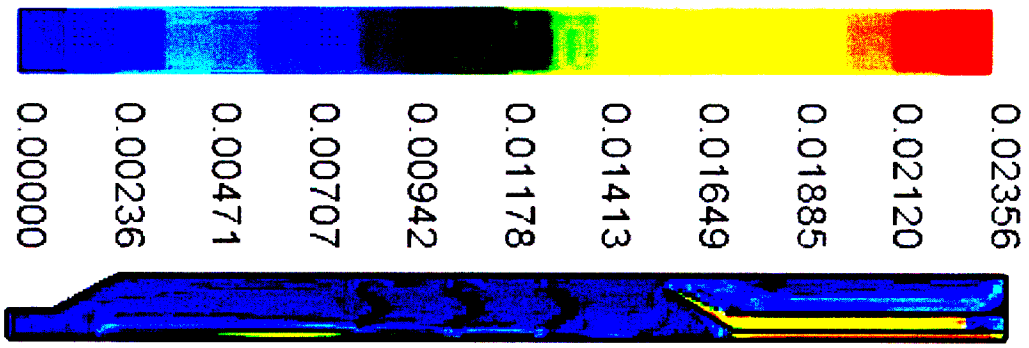

Figure 4.3-4: Velocity Contours (800µm Particles) [$m.s^{-1}$]

The majority of the 100μm sized particles, enter the outer annulus and exit at the top of the clarifier (Figure 4.3-1). The particles that do settle pass the collector cone, are attracted to the central axis because of the upward flow in the dewatering pipe. Only some of these solids move up the dewatering pipe (the volume fraction of solid in the dewatering pipe is about 0.02). This indicates that some particles will be sent to the feed as seeding flocs. The rest of the particles settle to the bottom of the clarifier.

Following Figure 4.3-3, a greater degree of settling can be seen for the 800μm particle simulation. Some solids hold-up seems to occur at the first consolidation cone, especially at the outer edge (on the left), since the gap at this point is narrower than the gap at the central axis. The velocity contours (Figure 4.3-4) show downward velocities of up to $0.017 m.s^{-1}$ along the center, due to solids settling. At the conical baffle, there is a region of slightly higher solids concentration, implying particle circulation in this area.

All the 3mm particles settle; none rise up the outer annulus (Figure 4.3-5). Furthermore, there is considerably less hold-up at the consolidation cones. The volume fraction of solid at the outer gap has a maximum of around 0.10 compared to 0.18 in the case of 800μm particles. The rapid settling of solids coupled with the upward flow of displaced fluid created movement in the lower regions of the clarifier (Figure 4.3-6). However, velocities here are very low (around $0.005 m.s^{-1}$).

4.4 FLOCCULATION MODELLING

The flocculation process occurring in the clarifier was modelled using Fluent. The behaviour of solid particles in the floc bed region was modelled in MATLAB to estimate the reaction rate constant (k-parameter).

4.4.1 FORMULATION OF A GENERAL MODEL

The flocculation process needed to be described mathematically in order to be incorporated into the Fluent model. The starting point was a basic equation which grew in complexity as the model involved.

4.4.1.2 ADDITION OF A THIRD SECONDARY PHASE

The area of interest is the region within the conical baffle, since the floc bed forms there. The bed operates in the following manner:

- Small particles enter the bed, where a high number of collisions result in particle growth.
- Some particles will experience minimal growth, remaining small enough to pass through the bed and exit through the overflow.
- The rest of the small particles attach themselves to existing floc particles
    - Large flocs drop out of the bottom of the bed
    - Intermediate sized flocs remain in the bed

Hence, modelling of the floc bed requires particles that follow three different trajectories within the clarifier (sink or rise from the bed, or remain within the bed). The small and large particles were arbitrarily selected as 100μm and 8mm, respectively. Discrete phase modelling showed that a range of particle sized would circulate within the conical baffle but, using two-phase modelling, it was found that a secondary phase particles with a diameter of 2mm remained within the bed region (Figures 4.4-1 and 4.4-2). In these simulations, the bed region was spiked with 2mm particles and their behaviour observed.

The introduction of a third, intermediate size enabled the Fluent model to represent the three different particle trajectories more accurately. However, this increased the complexity of the flocculation kinetics. Now, small and medium particles combine to form medium ones, while medium particles combine to form large ones. As a result, two rate constants were required.

small + medium = medium
medium + medium = large

small solid fraction:	$mass\ source = -k_1 V_S V_M$	4.4.1-3
large solid fraction:	$mass\ source = k_2 V_M^2$	4.4.1-4
medium solid fraction:	$mass\ source = k_1 V_S V_M - k_2 V_M^2$	4.4.1-5

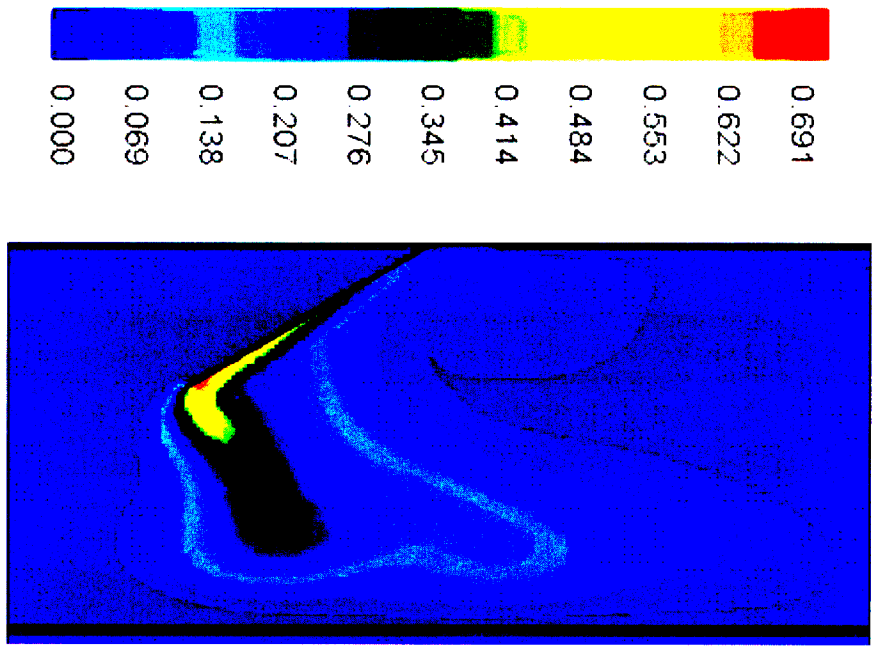

Figure 4.4-1: 2mm Particle Behaviour (800s) [volume fraction]

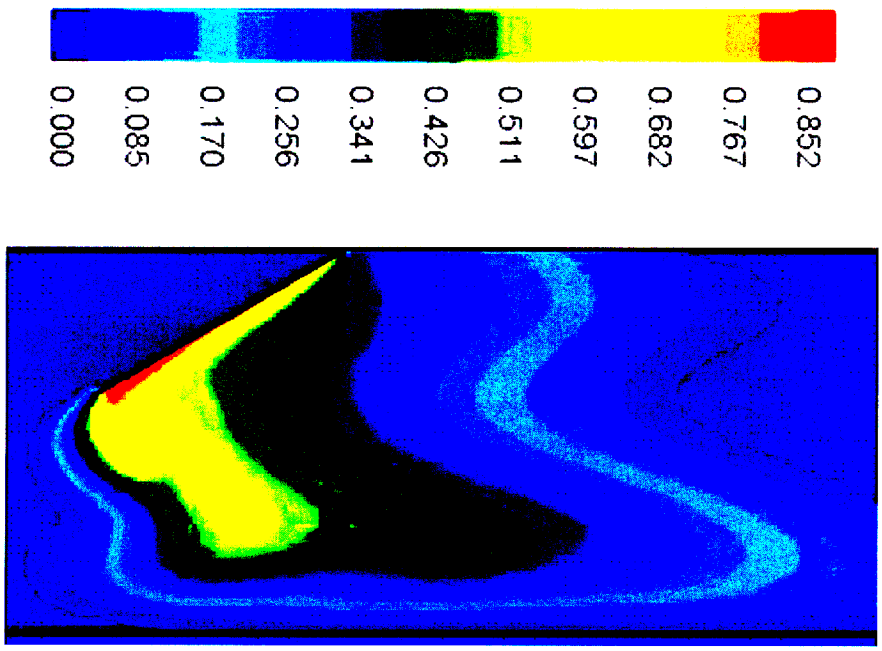

Figure 4.4-2: 2mm Particle Behaviour (7200s or 2hours) [volume fraction]

4.4.1.3 A MODIFIED KINETIC

The problem with the above scheme was the addition of a new variable (k_2). To avoid the difficulties in estimating this rate constant, another scheme was formulated. It contains all three solid size fractions, but only one rate constant; now, small particles and medium sized particles combine to form large ones.

small + medium = large

small solid fraction:	$mass\ source = -kV_S V_M$	4.4.1-6
medium solid fraction:	$mass\ source = -kV_S V_M$	4.4.1-7
large solid fraction:	$mass\ source = 2kV_S V_M$	4.4.1-8

Simulations were then run with the same boundary conditions as before. The feed composition was 5% 100μm, 5% 2mm and 0% 8mm solid phase, and, the value of k was now set to $100 kg.m^{-3}.s^{-1}$. Once again the bed region was spiked with 2mm particles. Figures 4.4-6, 4.4-7 and 4.4-8 show the resulting solid phase distributions after 6000s (100minutes).

The simulation results are similar to those obtained in the earlier model. The rate constant, controlling the formation of large particles is higher now, resulting in some of the large solid phase evolving in the mixing chamber (Figure 4.4-8).

4.4.2 CSTR MODEL IN MATLAB

The bed of flocculated particles is the feature of most interest in this design. Particles within the bed experience a high degree of mixing due to circulating flows as well as differential settling of solids. This led to the idea of modelling the floc bed as a perfectly mixed reactor (continuous stirred tank reactor – CSTR) within the MATLAB simulation package. MATLAB requires less iteration time due to the simplicity of the model, and can therefore provide quick estimates of the rate constant, k. The processes of floc capture and growth using the same flocculation kinetics utilised in the Fluent model are included in this model. Settling is incorporated into the model using the standard fluid mechanics equations. The model inputs are obtained from one of the experimental mixed juice runs at Maidstone Sugar Mill, Tongaat (20-11-2003 – run 1 – Graph C-4).

4.4.2.1 MODEL SIMPLIFICATIONS

- The volume within the conical baffle is considered to be the bed volume. Since the bed formed in the clarifier is suspended by the upward flow, it can, in reality, expand and is not confined to this volume. However, the Fluent simulations show that expansion of the bed is minimal with most of the 2mm phase remaining within the baffle.
- The bed is perfectly mixed. This implies that the volume fractions of each phase are the same, everywhere in the bed. This is a reasonable assumption for the medium and small solid phases as these size fractions do tend to distribute somewhat evenly throughout most of the bed region. This can be seen in the Fluent model solids distributions. However, these simulation results also reveal that the outer regions of the bed have almost no large solid phase present. Consequently, the flocculation modelling is affected, since floc capture as well as growth rates depend on the volume fraction of the large phase.
- The model uses a settling equation based on the assumption that the particle is a single body settling in a fluid, but at the bottom of the bed, a high concentration of large solids means that particle-particle interactions are not negligible.
- The feed solids volume fraction is obtained from the sample taken below the bed during pilot plant experiments. It cannot be determined what fraction of the solids,

$$u_t = \sqrt{\frac{4gd_p(\rho_p - \rho)}{3\rho C_D}} \qquad 4.4.3\text{-}2$$

where:

u_t is the terminal settling velocity

g is the gravitational acceleration ($9.8 m.s^{-2}$)

d_p is the particle diameter

ρ_p is the solid particle density

ρ is the fluid (juice) density

The final terminal velocity (of 8mm particles) was calculated to be $0.0134 m.s^{-1}$. The volume fraction of the small solid phase in the feed was set to 0.017 (a value obtained by analysing a sample, taken below the conical baffle). Using the cross-sectional area at the bottom of the conical baffle and the settling velocity of 8mm (large) spheres along with the solid density, the settling factor for the large solids fraction was determined.

$$settling\ factor = \rho_s A u_t \qquad 4.4.3\text{-}3$$

where:

A is the cross sectional area at the bottom of the bed

u_t is the 8mm particle terminal settling velocity

Vectors for the storage of time, volume fractions and average volume fractions were initialised (zero vectors). Thereafter, the program finds the steady state volume fractions for each solid phase for a range of k (flocculation rate kinetic) values (1 to $50 kg.m^{-3}.s^{-1}$). The time interval is one second and iterations continue for 8000 seconds (133.3 minutes). At each time interval, the mass change for each size fraction is found using the current volume fractions. The processes that contribute to the changes in volume fraction are flocculation, the settling of large flocs, and, the escape of small flocs that rise through the bed. The average volume fractions over the last 400 seconds (6.7 minutes) are stored for each value of k.

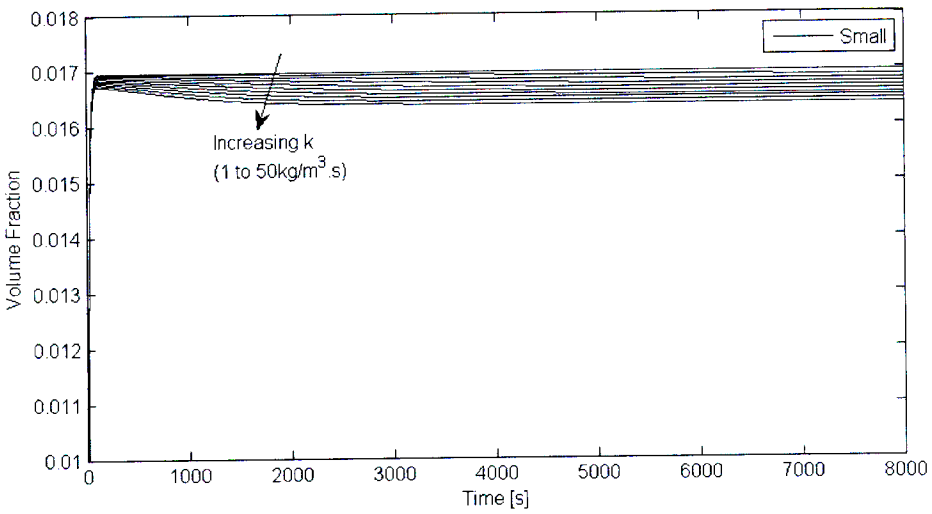

Graph 4.4-1: Volume Fraction Profile of Small Sized Particles for Varying k

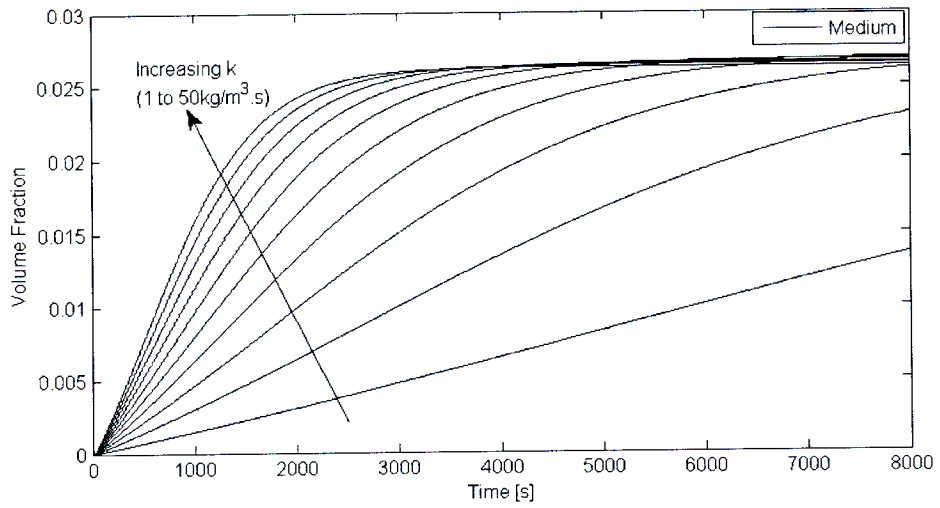

Graph 4.4-2: Volume Fraction Profile of Medium Sized Particles for Varying k

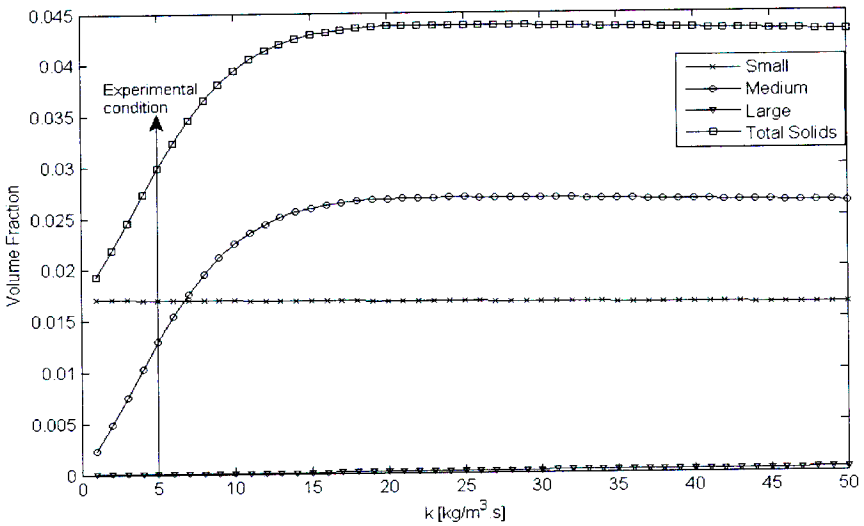

Graph 4.4-5: Steady State Volume Fractions Particles for Varying k

The MATLAB code was modified to assess the sensitivity of the system to the inlet solids volume fraction. Graphs 4.4-6 shows the resulting steady state volume fractions within the bed for small, medium, large and total solids. At a constant k of $5kg.m^{-3}.s^{-1}$, it was found that increasing the amount of small solids entering the system caused an increase in the steady state concentrations of all particles.

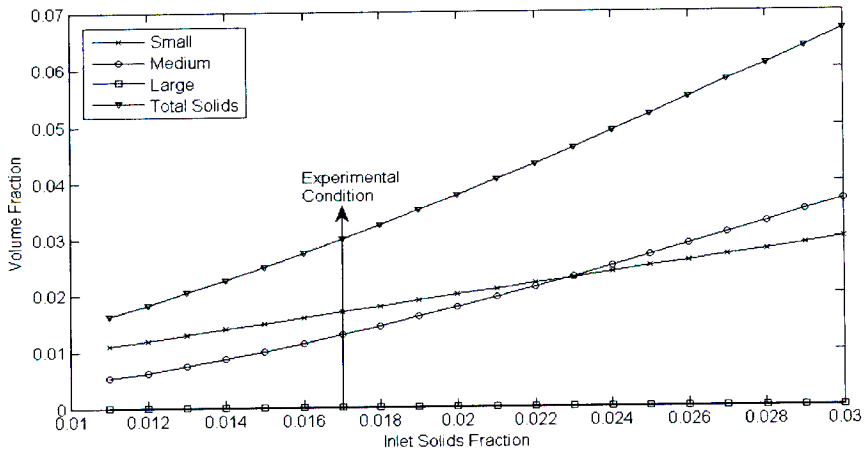

Graph 4.4-6: Steady State Profiles for Varying Inlet Solids Concentration

CHAPTER 5 DISCUSSION

Results of the clarifier experiments and CFD modelling were discussed earlier in **Chapter 3 and Chapter 4** respectively. This chapter serves as a summary of those previous discussions, and forms the basis for the conclusions and recommendations that follow in **Chapter 6.**

5.1 EXPERIMENTAL

Practical evaluation of the new clarifier design was conducted on the laboratory scale Magra Ultrasep clarifier. There were three sets of experiments; two at Maidstone Sugar Mill and one at the University of Kwa-Zulu Natal (Durban campus). The main aims of these experiments were firstly, to see if the clarifier could in fact be used for mixed juice clarification, and secondly, to obtain parameter values required in the CFD model. The steady state volume fractions at various points within the clarifier were specifically required to estimate the rate constant (k) using the Matlab CSTR model. This would be incorporated into the CFD model, which can then be calibrated by modelling a different set of conditions and confirming the result experimentally. The outcome would be a CFD model that can be modified to find the optimum parameters and/or geometry for effective use of the Magra Ultrasep in mixed juice clarification.

5.1.1 MAIDSTONE 2002

The lab scale clarifier was taken to Maidstone and fed with the same flocculated sugar cane juice that enters the Rapi-Dorr clarifier. The initial method of measuring solids content was found to be unreliable. The absorbance reading from a spectrophotometer was unsuitable for the samples with a large fraction of solids, frequently experienced at various points in the Magra Ultrasep clarifier.

High solids content in the feed frequently caused the rotameter to get stuck, making the flow reading unreliable. Thereafter, the rotameter had to be moved to measure the overflow rate instead.

The performance of the clarifier during these tests was erratic; therefore, the best data set was selected to determine the model parameter in **Chapter 4**.

5.2 CFD MODELLING

This discussion revolves around the development of the CFD model in the Fluent program.

First, the clarifier hydrodynamics were solved in the Fluent program. A circular flow pattern was observed in the region just above the conical baffle. The possibility of a bed of suspend flocs in this area was further confirmed using discrete phase modelling. Particles of various sizes were injected into the clarifier model feed stream. The particle trajectories showed that the larger particles settled, while smaller particles left through the overflow, or circulated in the dewatering pipe. Further particle injections above the conical baffle resulted in particles with diameters between 100μm and 4mm circulating in this region.

A two-phase model was created with solids and liquid entering together in the feed. For three different sized solids fractions, a different behaviour was observed in the clarifier. The effect of flocculation was integrated into the model by using various solid phases and changing the volume fraction of each according to a rate equation. This equation was in the form of a classical reaction kinetic, with the rate of transfer from one solid phase to another dependent on the volume fraction (concentration) and a rate constant. This constant was calculated using the data acquired from the Maidstone 2003 experiment. A continuous stirred tank reactor (CSTR) model was set up on MATLAB to simulate the behaviour of the bed of circulating flocs. Floc growth as well as particle settling is taken into account. Various values for the k parameter (reaction rate constant) are input and the model solves for the steady state particle size distributions. A value of $5 kg.m^{-3}.s^{-1}$ results in the required total solid volume fraction of 0.03. It should be noted that since only one experimental data set was used, this value for the k parameter is not reliable.

CHAPTER 6 CONCLUSIONS AND RECOMMENDATIONS

This chapter discusses the conclusions and recommendations arising from the discussion of experimental and modelling results presented in **Chapters 3** and **4** respectively.

6.1 CONCLUSIONS

- The Magra Ultrasep did not perform as well as expected; when run in parallel with the Rapi-Dorr, the old clarifier outperformed the new design. However, the issues mentioned above need to be resolved before making a more definite conclusion concerning its suitability for sugar cane juice clarification.

- The key aspect of this clarifier design is the suspended bed of circulating floc particles. According to CFD simulations, this bed will form in the region above the conical baffle, as per the design intent of the Magra Ultrasep. This was also confirmed experimentally, especially during the Maidstone 2003 experimental run.

- The value of the k-parameter (flocculation rate reaction constant) was calculated to be $5kg.m^{-3}.s^{-1}$. However, since this was based on a single experimental run, this result is not reliable. The procedure used is merely a demonstration of how this parameter could be calculated for a given set of conditions. As explained in the discussion, evaluating the k-parameter and testing various model conditions followed by experimental confirmation will produce a calibrated CFD model.

- The flocculation process was successfully integrated into the CFD model. The model was simplistic, but could possibly form the framework for building a more complex model, that, once calibrated will be able to predict clarifier performance.

Model parameters for Fluent need to be calculated using reliable, reproducible data. Greater experimental stability, as described in the two points above will enable this.

- The flocculation model used in Fluent needs to be developed further, as only three size fractions are incorporated in the model. Population balance modelling might be the next step forward.

- The action of a manual, periodic solids removal needs to be investigated using the Fluent model. The effect that this will have on the bed of flocculated particles needs to be assessed.

- More information on the flocs themselves would be useful for model formulation e.g. floc shape, density and strength.

REFERENCES

ADAMS EW AND RODI W (1990). Modelling flow and mixing in sedimentation tanks. *Journal of Hydraulic Engineering, ASCE*, **116**(7), 895-913.

ARMBRUSTER M, KREBS P and RODI W (2001) Numerical modelling of dynamic sludge blanket behaviour in secondary clarifiers. *Water Sci. Tech.* **43** (11) 173-180.

BOUYER D, LINE A, COCKX A, and DO-QUANG Z (2001) Experimental analysis of floc size distribution and hydrodynamics in a jar-test. *Trans IChemE* **79** (Part A) 1017-1024.

BRANNOCK MWD, HOWES A, JOHNS M, DE CLERCQ B AND KELLER J (2002) CFD modelling of particle transport and biological reactions in a mixed wastewater treatment vessel. Information accessed on 20th August 2003 from: http://www.leapaust.com.au/services/casestudy/casestudy.htm

BRETSCHER U, KREBS P AND HAGER WH (1992). Improvement of flow in final settling tanks. *Journal of Environmental Engineering, ASCE*, **118**(3), 307-321.

BROUCKAERT CJ, HUANG T AND BUCKLEY CA (2005) Applications of Computational Fluid Dynamics Modelling in Water Treatment. *Report to the Water Research Commission by Pollution Research Group, University of Natal, Durban, SA.*

CAMP TR and STEIN PC (1943) Velocity gradients and internal work in fluid motion. *J. Boston Soc. Civ. Eng.* **30** 219-237.

CHATAIGNER O, GAGNON JL, CHAGNEAU G AND CHOPARD P (1999) FLUENT: modelling for optimising the design of post-chlorination tanks, *Houille Blanche-Revue Internationale de l'Eau,* **54** (3-4): 15-20

CHETTY S AND DAVIS SB (2001) CFD modelling of a Rapidorr 444 Clarifier: Recent progress. *Proc. S Afr. Sug. Technol.* **75** 298-302.

HAARHOFF J and VAN DER WALT JJ (2001). Optimal design parameters for hydraulic flocculators. *Journal of Water Supply: Research and Technology - AQUA*, **50**(3) 149-159.

JONES SC, SOTIROPOULOS F and AMIRTHARAJAH A of helical static mixers for water treatment. *Journal of Environmental Engineering* **128**(5) 431-440.

KAMIMURA M, FURUKAWA S AND HIROTSUJI J (2002). Development of a simulator for ozone/UV reactor based on CFD analysis. *Water Science and Technology*, **46**(11-12), 13-19.

KREBS P (1991). The hydraulics of final settling tanks. *Water Science and Technology*, **23**(4-6), 1037-1046.

LI X and GANCZARCZYK J (1989) Fractal geometry of particle aggregates generated in water and wastewater treatment processes. *Environ. Sci. Technol. 23* 1385-1389.

LYN DA AND RODI W (1990). Turbulence measurement in model settling tank. *Journal of Hydraulic Engineering, ASCE*, **116**(1), 3-21.

LYN DA, STAMOU AI AND RODI W (1992). Density currents and shear-induced flocculation in sedimentation tanks. *Journal of Hydraulic Engineering, ASCE*, **118**(6), 849-867.

MATKO T, FAWCETT N, SHARP A AND STEPHENSON T (1996). A numerical model of flow in circular sedimentation tanks. *Trans IChemE.*, **74**(B), 197-204.

MCCORQUODALE JA AND ZHOU S (1993). Effects of hydraulic and solids loading on clarifier performance. *Journal of Hydraulic Research, ASCE*, **31**(4), 461-478.

NOPENS I, BIGGS CA, DE CLERCQ B, GOVOREANU R, WILEN BM, LANT P and VANROLLEGHEM PA (2002) Modelling the activated sludge flocculation process combining laser light diffraction particle sizing and population balance modelling (PBM). *Water Sci. Technol.* **45** (6) 41-49.

STEINDL RJ (1995) Optimum performance through CFD modelling of clarifier designs. *Proc. Aust. Soc. Sugar Cane Technol.1995 Conf.* 207-215.

STEINDL RJ, FITZMAURICE AL, ALMAN CW (1998) Recent developments in clarifier design. *Proc. Aust. Soc. Sugar Cane Technol.* **20** 477-483.

SWIFT DL and FRIEDLANDER SK (1964) The coagulation of hydosols by Brownian motion and laminar shear flow. *J. Coll. Sci.* **19** 629.

TA CT, BECKLEY J AND EADES A (2001). A multiphase CFD model of DAF process. *Water Science and Technology* **43**(8) 153-157

TAKACS I, PATRY GG and NOLASCO D (1991) A dynamic model of the clarification-thickening process. *Wat. Res.* ***25*** (10) 1263-1271.

TAMBO N (1965) A fundamental investigation of floc growth (1). *J. Jpn. Water Works Assoc.* **372** 10-19.

TAMBO N and HOZUMI H (1979) Physical characteristics of flocs – II. *Strength of Floc. Water Res.* **13** 421.

THOMAS DN, JUDD SJ, FAWCETT N (1999) Flocculation Modelling: A Review. Water Res. 33 (7) 1579-1592

VERWEY EJW and OVERBEEK J Th G (1948) Theory of the stability of lyophobic colloids. *Elsevier, Amsterdam.*

ZHOU S AND MCCORQUODALE JA (1991). Influences of density on circular clarifiers with baffles. *Journal of Environmental Engineering, ASCE,* **118**, 365-374.

ZHOU S AND MCCORQUODALE JA (1992a). Mathematical modelling of a circular clarifier. *Canadian Journal of Civil Engineering*, **19**(3), 365-374.

APPENDIX A: MAIDSTONE 2002 EXPERIMENTAL RESULTS

A.1. CALIBRATION

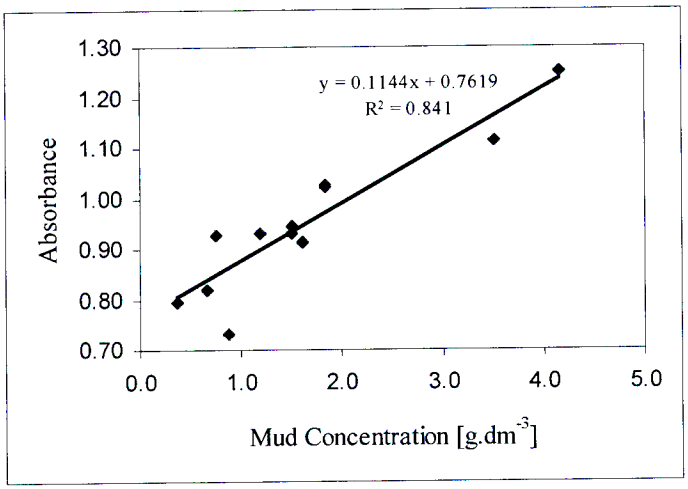

Graph A-1: Relationship between Absorbance and Mud Concentration for Mixed Juice

A.2. EXPERIMENTAL RESULTS

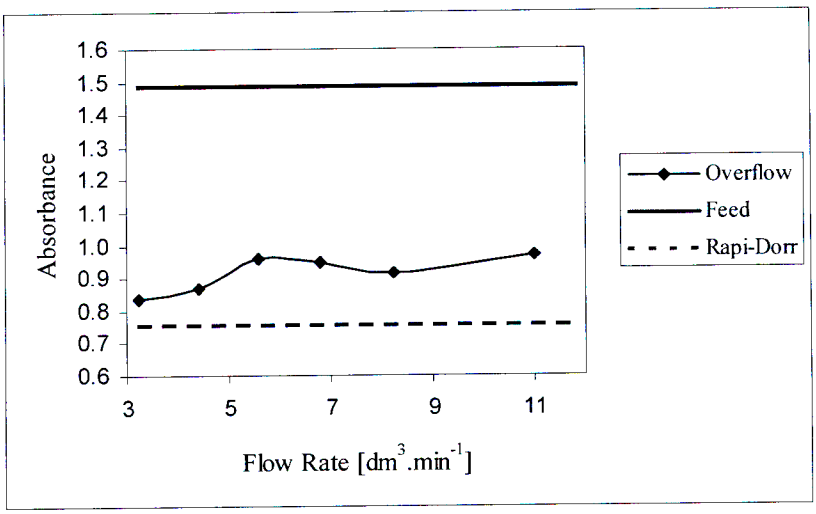

Graph A-2: Overflow Absorbance with Changing Flow Rate (22-11-2002)

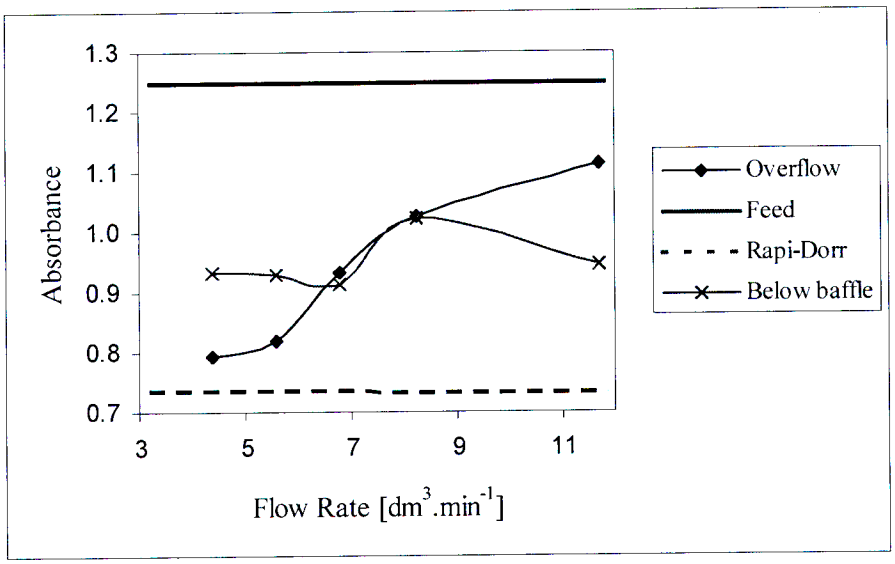

Graph A-5: Absorbances of the Overflow and Below the Baffle (27-11-2002 – run 1)

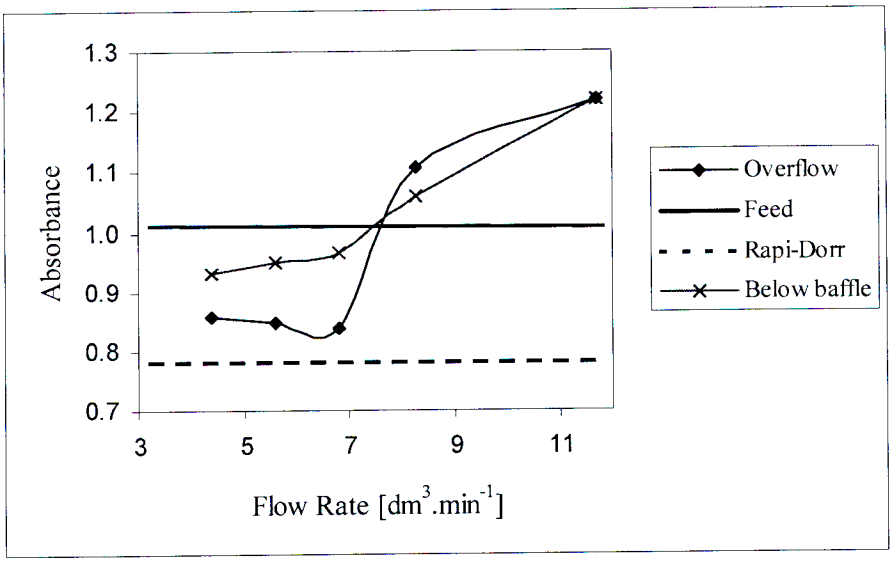

Graph A-6: Absorbances of the Overflow and Below the Baffle (27-11-2002 – run 2)

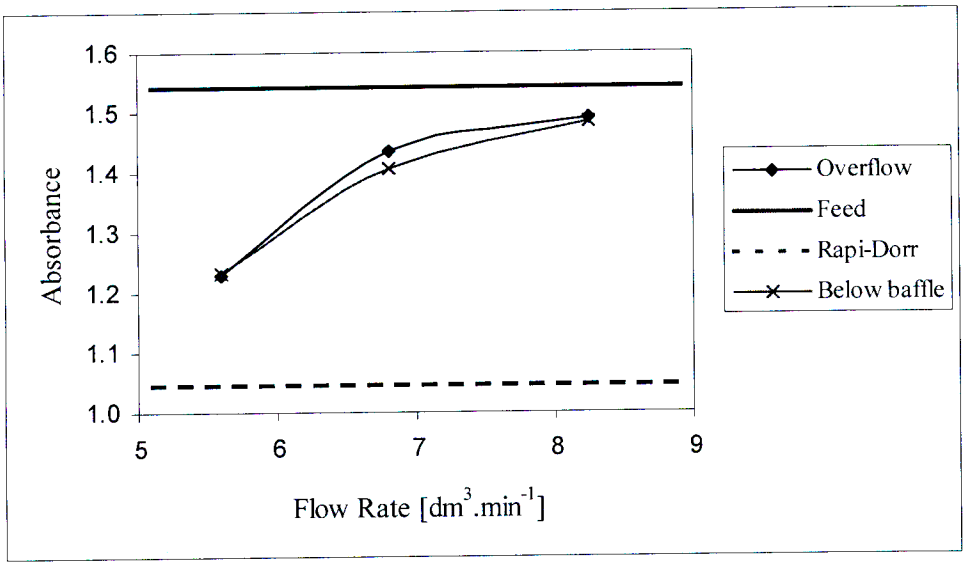

Graph A-9: Absorbances of the Overflow and Below the Baffle (02-11-2002 – run 2)

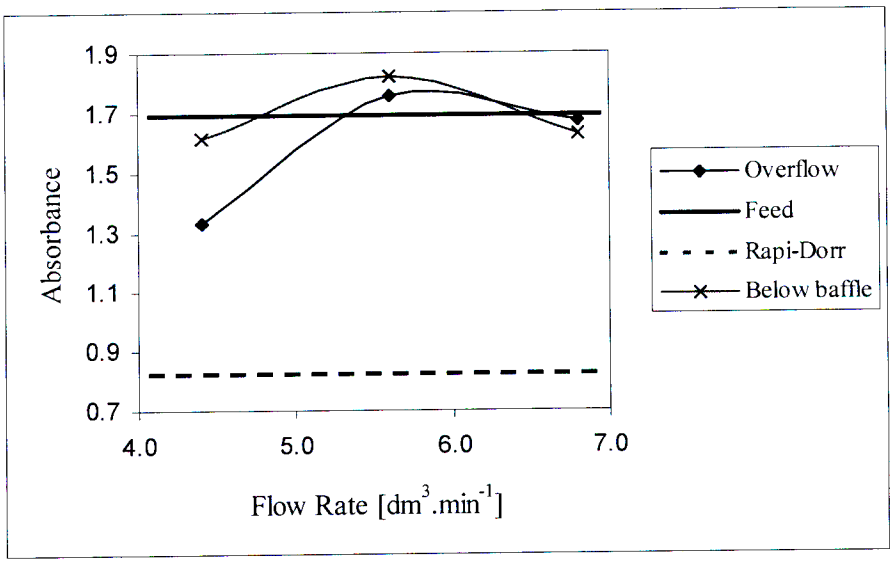

Graph A-10: Absorbances of the Overflow and Below the Baffle (03-11-2002)

APPENDIX B: ALUM EXPERIMENT RESULTS

B.1. CALIBRATION

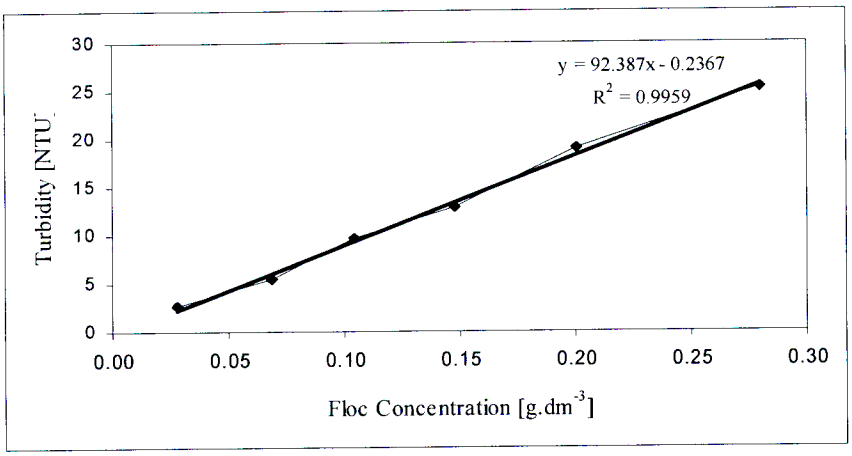

Graph B-1: Relationship between Turbidity and Floc Concentration in Water

B.2. EXPERIMENTAL RESULTS

Graphs B-2 to B-6 show the turbidities at the various sample points for a run time of 30minutes.

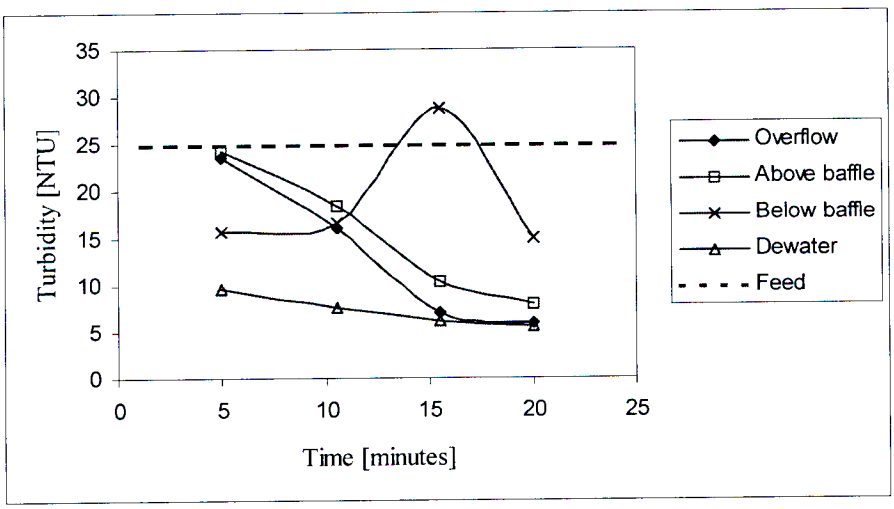

Graph B-2: Turbidity Profiles within the Magra Ultrasep (28-05-2003)

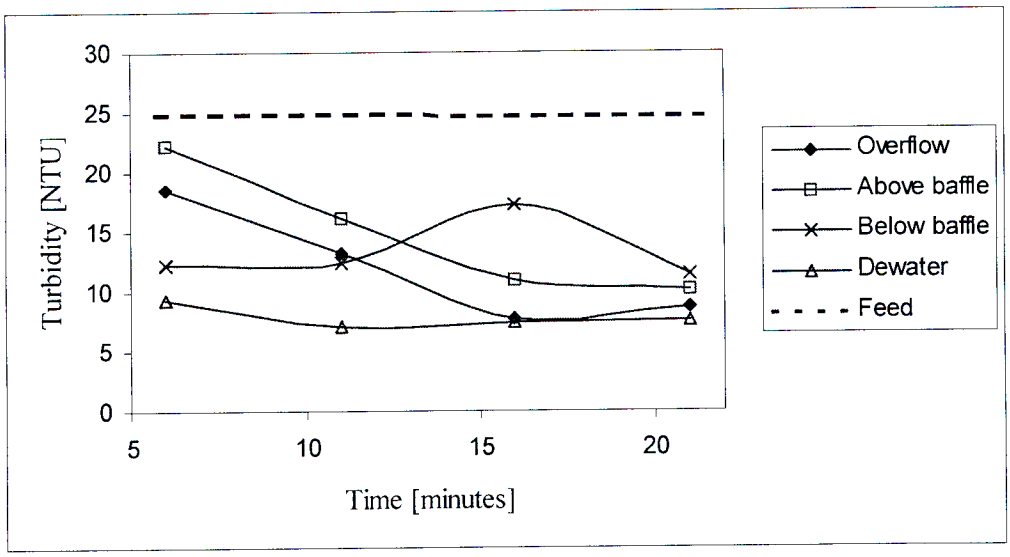

Graph B-5: Turbidity Profiles within the Magra Ultrasep (06-06-2003 – run 1)

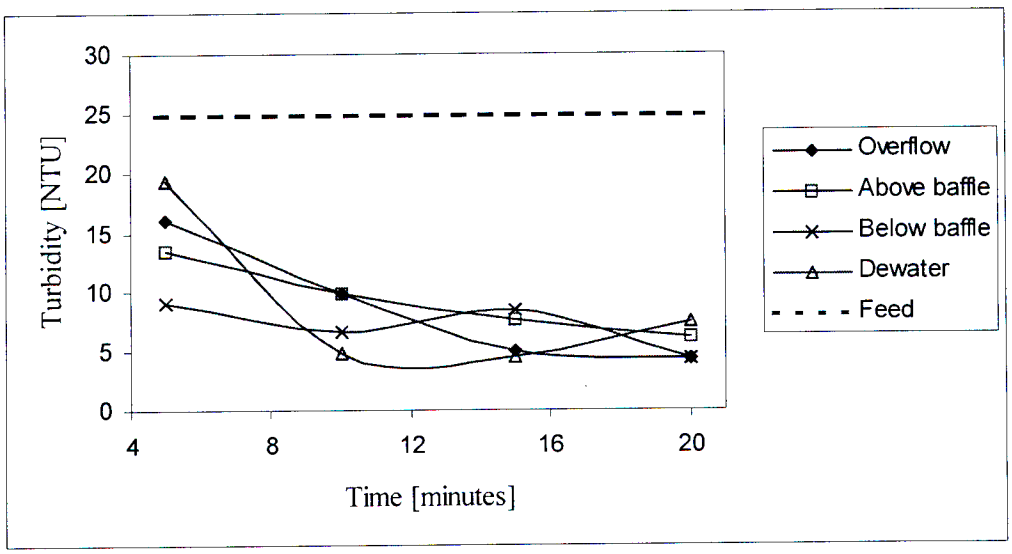

Graph B-6: Turbidity Profiles within the Magra Ultrasep (06-06-2003 – run 2)

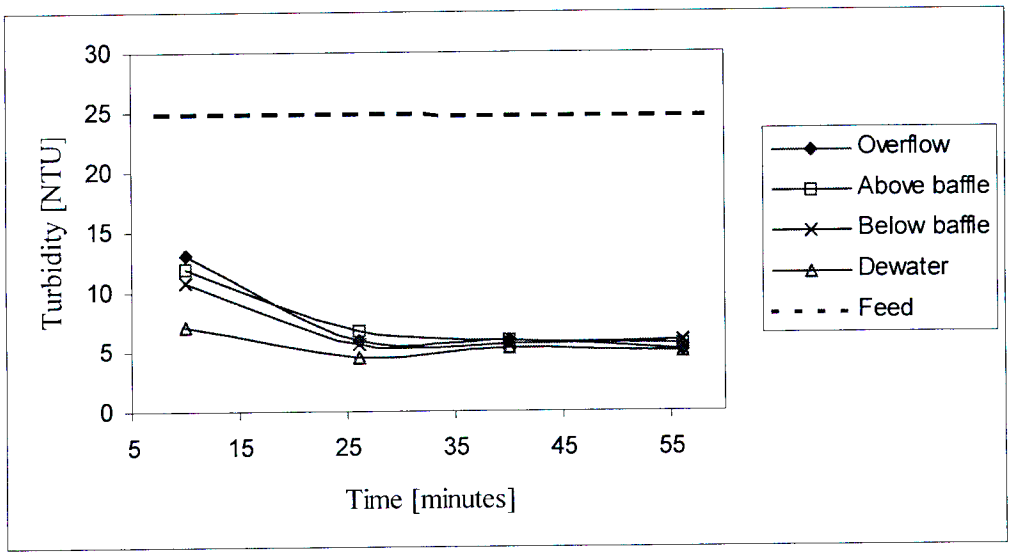

Graph B-9: Turbidity Profiles within the Magra Ultrasep (11-06-2003 – run 1)

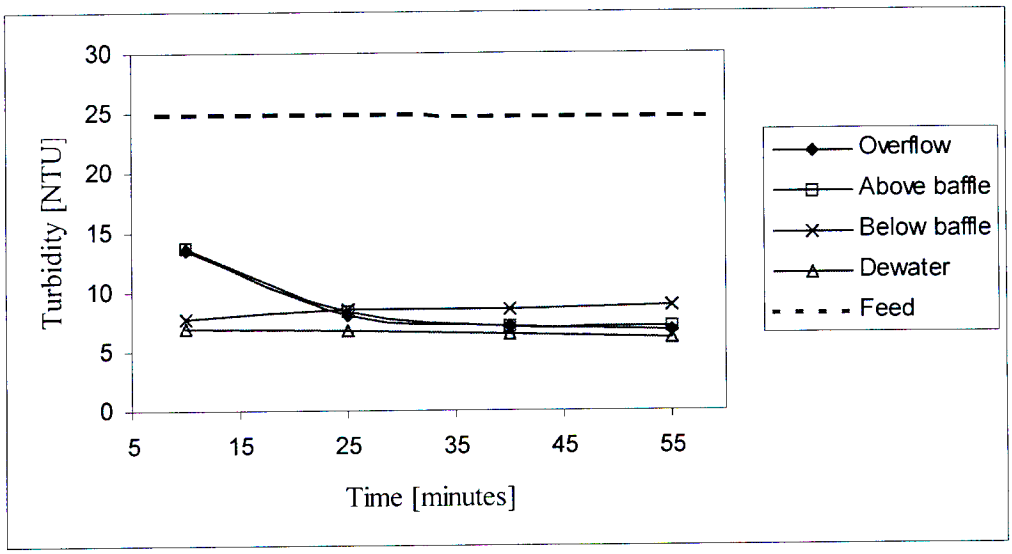

Graph B-10: Turbidity Profiles within the Magra Ultrasep (11-06-2003 – run 2)

Graphs B-13 to B-16 show the results of five hour runs.

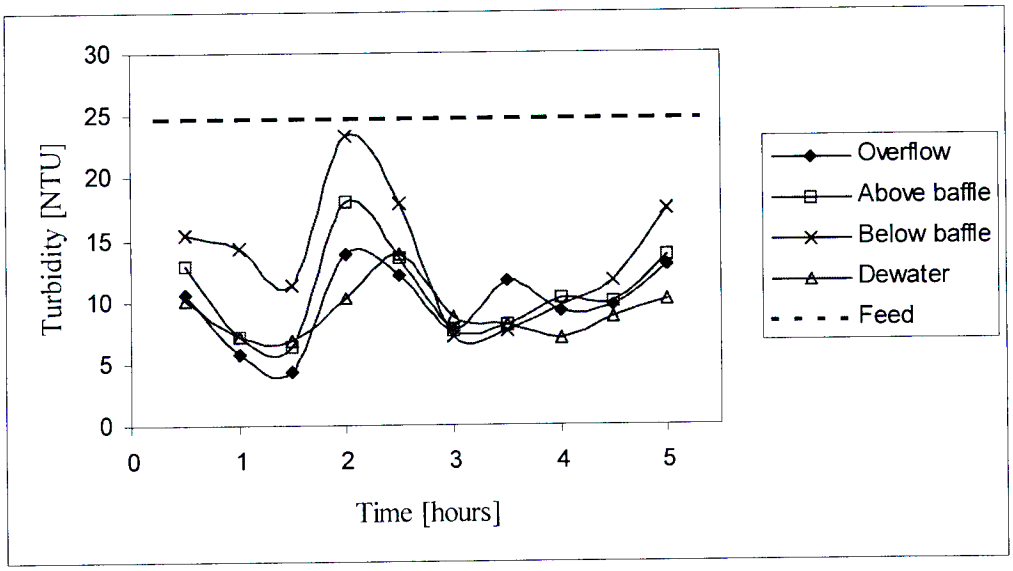

Graph B-13: Turbidity Profiles within the Magra Ultrasep for a 5hour run (10-07-2003)

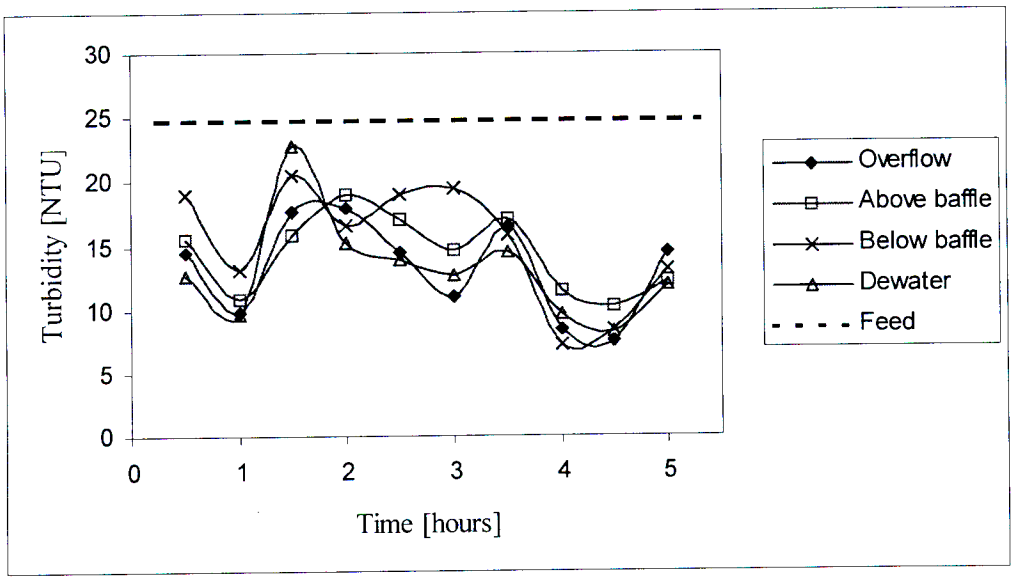

Graph B-14: Turbidity Profiles within the Magra Ultrasep for a 5hour run (16-07-2003)

APPENDIX C: MAIDSTONE 2003 EXPERIMENTAL RESULTS

C.1. EXPERIMENTAL RESULTS

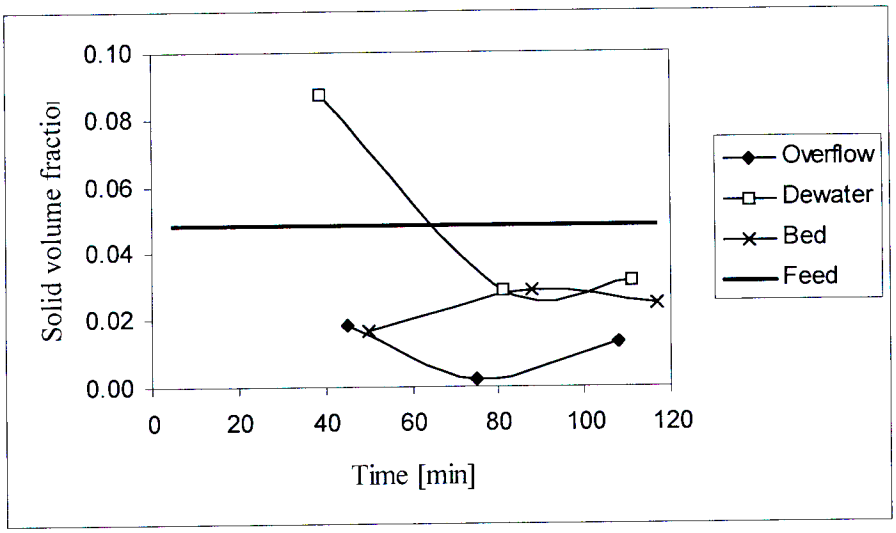

Graph C-1: Volume Fraction Profiles (18-11-2003 – run 1)

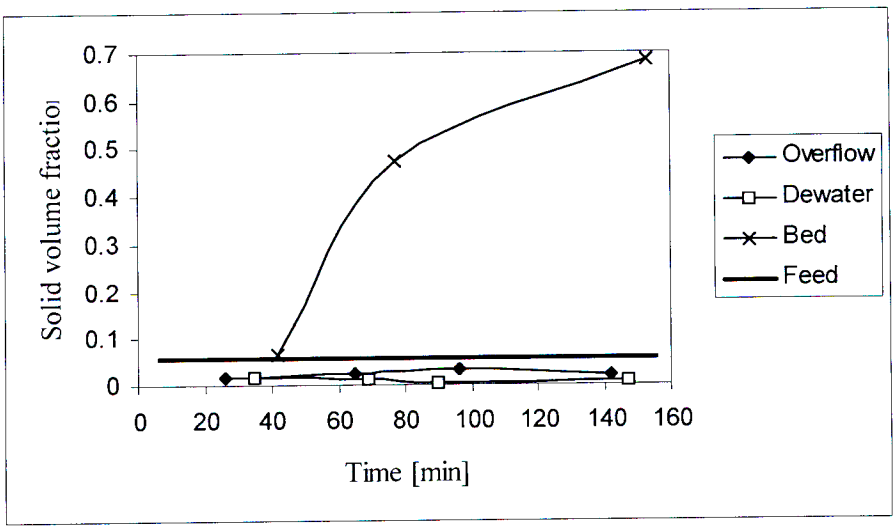

Graph C-2: Volume Fraction Profiles (18-11-2003 – run 2)

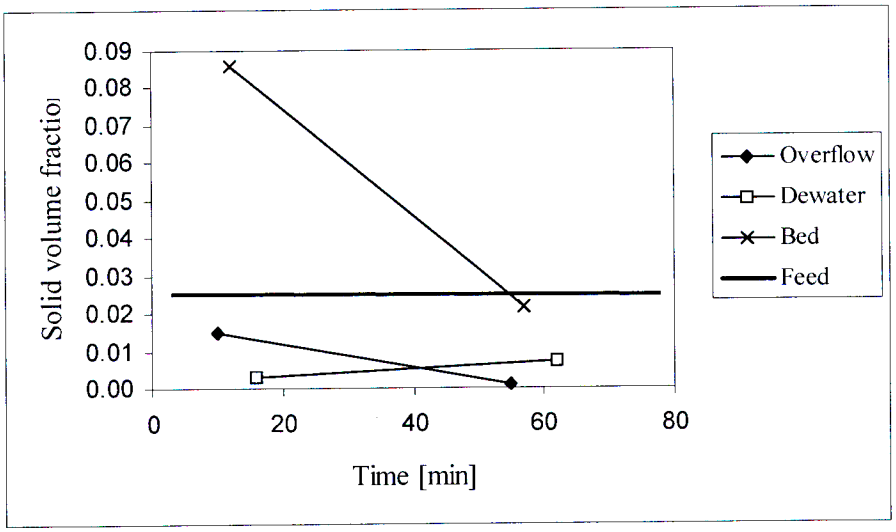

Graph C-5: Volume Fraction Profiles (20-11-2003 – run 2)

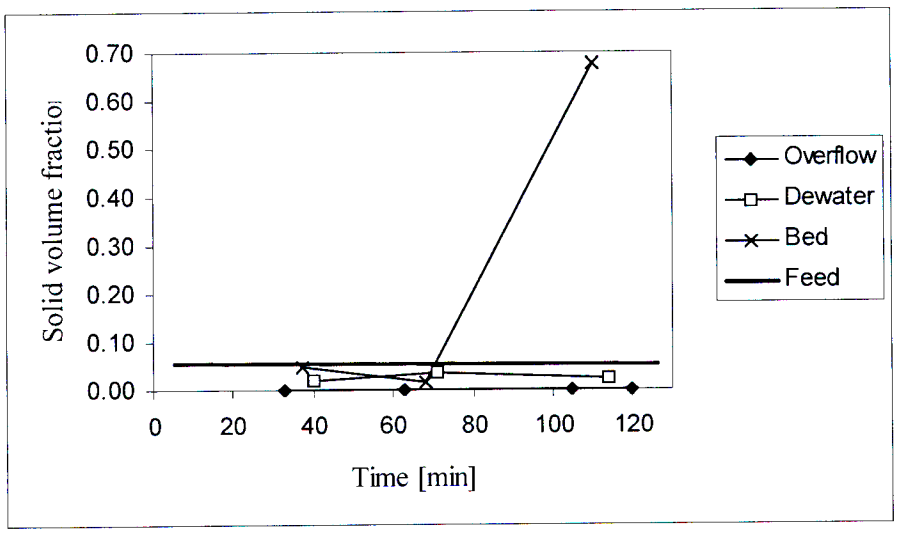

Graph C-6: Volume Fraction Profiles (21-11-2003 – run 1)

APPENDIX D: USER DEFINED FUNCTION USED IN FLUENT

This function, written in the C programming language, allowed a user defined function to effect flocculation in the Fluent model.

```
/************************************************************/
/* UDF for defining a mass source within each cell          */
/************************************************************/
#include "udf.h"
#define k 10

DEFINE_SOURCE(s_source, cell, this_thread, dS, eqn)
{
Thread *mixture_thread;
Thread **pt;
real  vs, vm, vl, source;

mixture_thread = THREAD_SUPER_THREAD(this_thread);
```

```
mixture_thread = THREAD_SUPER_THREAD(this_thread);

pt = THREAD_SUB_THREADS(mixture_thread);

vs = C_VOF(cell, pt[1]);

vl = C_VOF(cell, pt[3]);

vm = C_VOF(cell, this_thread);



source = -k*vm*vs;

dS[eqn] = -k*vs;



return source;

}



DEFINE_SOURCE(l_source, cell, this_thread, dS, eqn)

{

Thread *mixture_thread;

Thread **pt;

real  vm, vs, source;
```

APPENDIX E: MATLAB PROGRAM FOR K-PARAMETER ESTIMATION

```
% PROGRAM TO SIMULATE A PERFECTLY MIXED FLOC BED IN MAGRA
ULTRASEP CLARIFIER

%Select control volume to be the total cone volume
%Vol of cone - formula obtained by integration method
h = 0.052;
r_in = 0.1;
r_out = 0.13;
r_feed = 0.055;
vol = pi*r_out^2*h - pi*h*(1/3*(r_in-r_feed)^2+r_feed*(r_in-r_feed)+r_feed^2);

% Volumetric flow rate of feed
flow_fluid = 6/(1000*60);  % m3/s - set at 6dm3/min

% densities [kg/m3]
rho_fluid = 998.2;
rho_solid = 1000;

% upward velocity of fluid
upvel_cyl = flow_fluid/(pi*(r_out^2-r_feed^2));

% assumption- solid vol frac below bed indicates condition of feed into cone
% Vol frac of solid below cone - (run 1 value) for 20/11/2003
v_below = 0.017;

% inlet flow rates of solid particles into bed (from feed) [kg/s]
% feed is composed of small particles only
flow_s_in = (v_below*flow_fluid*rho_solid);

% cone bottom area [m2]
A = pi*(r_out^2-r_in^2);
upvel_cone = flow_fluid/A;

% gravitional acceleration - m/s2
g = 9.8;

% 8mm particle terminal velocity calculated by hand
u_term_8mm = 0.0134;
setvel_8mm = u_term_8mm - upvel_cone;

% particle settling factor [kg/(m3.s)]
set_factor = rho_solid*setvel_8mm*A;
```

```
    % determine volume fraction from mass
    Vs(j,i) = (mass_s(i)/rho_solid)/vol;
    Vm(j,i) = (mass_m(i)/rho_solid)/vol;
    Vl(j,i) = (mass_l(i)/rho_solid)/vol;
    Vtot(j,i) = Vs(j,i) + Vm(j,i) + Vl(j,i);
end

% find average volume fractions over the last 400 seconds or 6.7 minutes
sum_s = 0;
sum_m = 0;
sum_l = 0;
for n = (t_iter-800/dt):t_iter
    sum_s = sum_s + Vs(j,n);
    sum_m = sum_m + Vm(j,n);
    sum_l = sum_l + Vl(j,n);
end
avg_s(j) = sum_s/(800/dt);
avg_m(j) = sum_m/(800/dt);
avg_l(j) = sum_l/(800/dt);
avg_tot(j) = avg_s(j)+avg_m(j)+avg_l(j);

end


% DISPLAY CODE

for j = 1:10
    xi = j*5;
    plot(time,Vs(xi,:),'k');
    hold on;
end
xlabel('Time [s]');
ylabel('Volume Fraction');
legend('Small');
hold off;


figure;
for j = 1:10
    xi = j*5;
    plot(time,Vm(xi,:),'k');
    hold on;
end
xlabel('Time [s]');
ylabel('Volume Fraction');
legend('Medium');
hold off;
```

APPENDIX F: THE CLARIFICATION PROCESS IN SUGAR INDUSTRY

Sugar cane juice is extracted by first shredding the cane, followed by cane diffusion and dewatering. The subsequent clarification process removes the insoluble, soluble and colloidal impurities present in the juice. Heat and lime are added to the mixed juice, resulting in coagulation. The most important constituent of the mixed juice is sucrose. This can be lost by the action of micro-organisms or by chemical inversion, which is the hydrolysis of sucrose to form fructose and glucose. The equation is as follows:

$$C_{12}H_{22}O_{11} + H_2O \rightarrow C_6H_{12}O_6 + C_6H_{12}O_6$$

Low pH and high temperatures increase the rate of this reaction.

The key aspect of cane juice clarification is the formation of a voluminous precipitate that settles and traps other coagulated material. This is accomplished by the reaction of lime with phosphates present in the mixed juice to form the precipitates of octa-calcium phosphate and hydroxyapatite. The addition of lime also raises the juice pH from slightly acidic to neutral (or slightly alkaline), allowing for the formation of the calcium phosphate precipitate, as well as inhibiting the inversion reaction (sucrose degradation). Heating of the juice above 75°C (normally to about 100°C) prevents micro-organisms from consuming the sucrose. Furthermore, the rate of reaction phosphates with lime to form a precipitate is greatly increased.

Subsequent to liming, a polymeric flocculant (in this case polyacrylamide) is added to the mixed juice to enhance clarification. Mud particles attach onto the polymer chain's active sites. Consequently, the chains stick together forming larger floc particles, resulting in quicker solids settling rates.

Upon settling, flocculated mud can accumulate in clarifier mud compartments. Micro-organisms flourish in these regions resulting in deteriorating sugar quality. Lactic acid

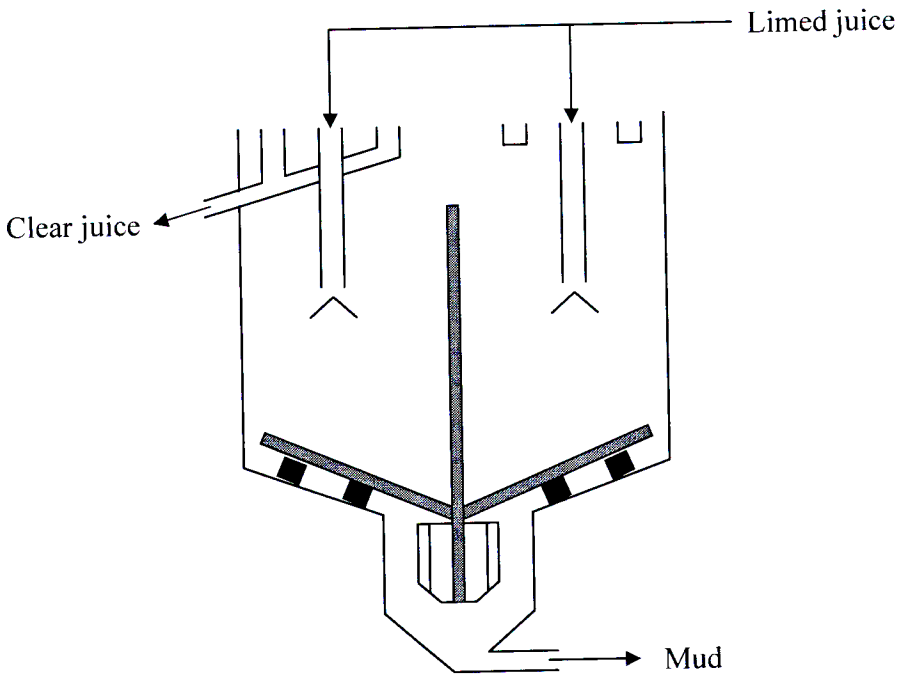

Figure F-2: SRI Clarifier

APPENDIX G: CLARIFIER DRAWINGS

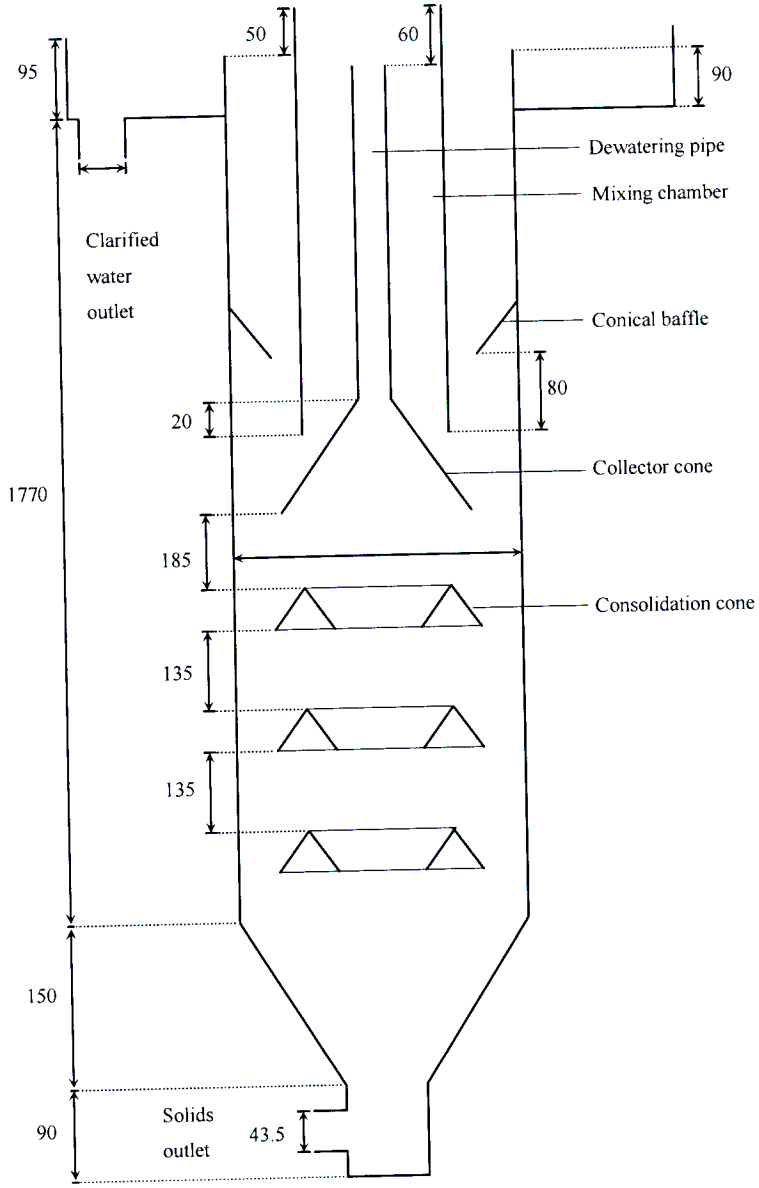

Figure G-1: Laboratory scale Magra Ultrasep 2000 Clarifier

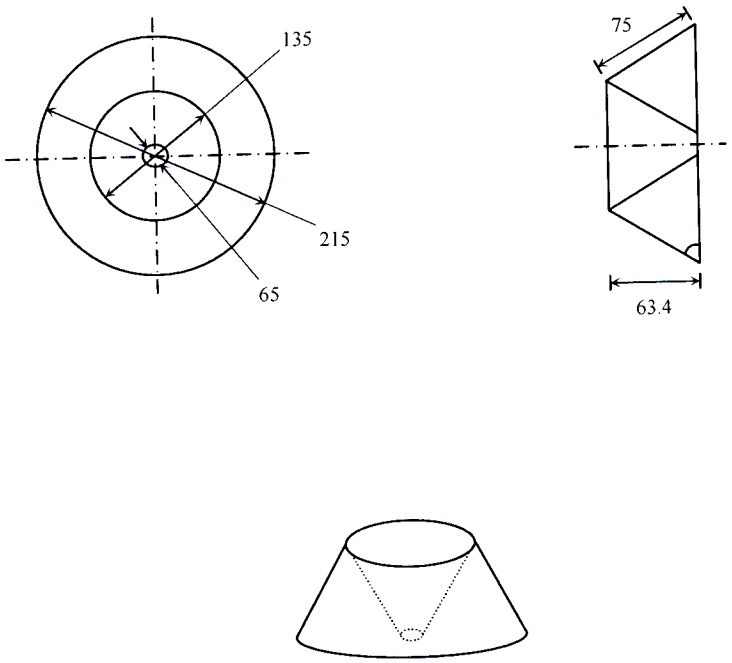

Figure G-5: Consolidation Cone